The Plant Cell, Vol. 8, 213–239, February 1996

Ovule Development: Identification of Stage-Specific and Tissue-Specific cDNAs

Jeanette A. Nadeau,[1] Xian Sheng Zhang,[2] Juan Li, and Sharman D. O'Neill[3]

Division of Biological Sciences, Section of Plant Biology, University of California at Davis, Davis, California 95616

A differential screening approach was used to identify seven ovule-specific cDNAs representing genes that are expressed in a stage-specific manner during ovule development. The Phalaenopsis orchid takes 80 days to complete the sequence of ovule developmental events, making it a good system to isolate stage-specific ovule genes. We constructed cDNA libraries from orchid ovule tissue during archesporial cell differentiation, megasporocyte formation, and the transition to meiosis, as well as during the final mitotic divisions of female gametophyte development. RNA gel blot hybridization analysis revealed that four clones were stage specific and expressed solely in ovule tissue, whereas one clone was specific to pollen tubes. Two other clones were not ovule specific. Sequence analysis and in situ hybridization revealed the identities and domain of expression of several of the cDNAs. O39 encodes a putative homeobox transcription factor that is expressed early in the differentiation of the ovule primordium; O40 encodes a cytochrome P450 monooxygenase (CYP78A2) that is pollen tube specific. O108 encodes a protein of unknown function that is expressed exclusively in the outer layer of the outer integument and in the female gametophyte of mature ovules. O126 encodes a glycine-rich protein that is expressed in mature ovules, and O141 encodes a cysteine proteinase that is expressed in the outer integument of ovules during seed formation. Sequences homologous to these ovule clones can now be isolated from other organisms, and this should facilitate their functional characterization.

INTRODUCTION

Throughout the history of plant biology, much attention has centered on the angiosperm ovule because of the central role played by the ovule in plant reproduction and agriculture. The ovule produces the female gametophyte, which gives rise to the haploid egg cell during plant sexual reproduction. The ovule also consists of sporophytically derived tissues that nourish and protect the female gametophyte and developing embryo. Ultimately, the mature embryo, endosperm, and maternal tissues of the ovule form the seed (Bouman, 1984).

The study of ovule development promises to yield valuable insights into general developmental mechanisms because many of the processes involved in ovule development have parallels in other eukaryotic organisms, including the establishment of polarity and pattern, lineage-specific cell and nuclear division, and programmed cell death (Drubin, 1991; St. Johnson and Nüsslein-Volhard, 1992; Martin et al., 1994). In the ovule, these processes are exemplified by events such as the redistribution of organelles and biochemical activities in the megasporocyte and female gametophyte during development, precisely regulated divisions of the megaspore nucleus and the construction of new cell walls in highly organized patterns within the female gametophyte, and the death of the three abortive megaspores or the death of integument cells to form the seed coat (Bouman, 1984; Noher de Halac and Harte, 1985; Huang and Russell, 1992).

Despite the wealth of descriptive knowledge concerning ovule anatomy and morphology, little is known about the molecular basis of ovule development and function. The relative inaccessibility of the ovule within the ovary and the difficulty in harvesting adequate amounts of tissue at known developmental stages have impeded progress toward understanding the molecular basis of ovule development and function. In an effort to understand these processes, several mutations affecting ovule and female gametophyte development have been identified, including *bell* (*bel1*), *short integuments* (*sin1*), *ovule mutant-2* (*ovm2*), and *ovule mutant-3* (*ovm3*), which cause female sterility in Arabidopsis (Robinson-Beers et al., 1992; Reiser and Fischer, 1993; Modrusan et al., 1994). Other genes shown recently to be involved in ovule development are *aberrant testa shape* (*ats*) (Léon-Kloosterziel et al., 1994) and *superman* (*sup*) (Gaiser et al., 1995), which regulate growth and differentiation of the integument. A few mutations defective in aspects of megasporogenesis also have been identified, such as the *megasporogenesis* (*msg*) gene in wheat (Joppa et al., 1987), *synaptic mutant-2* (*sy-2*) in *Solanum* (Parrott and

[1] Current address: Department of Plant Biology, Ohio State University, 1735 Neil Avenue, Columbus, OH 43210-1293.
[2] Current address: Section of Botany, Shandong Agricultural University, Taian, Shandong, 271018, People's Republic of China.
[3] To whom correspondence should be addressed.

Hanneman, 1988), and *female gametophyte factor* (*Gf*) in Arabidopsis (Rédei, 1965).

Little progress has been made in identifying and analyzing genes expressed specifically in the ovule and female gametophyte. A major goal of our research has been to develop a biological system in which it would be possible to isolate large quantities of synchronized ovules for the identification of ovule-specific and developmental stage–specific mRNAs. In many orchid species, no ovules are present in the ovary before pollination and instead are induced to develop by hormonal signaling associated with the pollination event (Zhang and O'Neill, 1993). Because of the precise manner in which the ovule developmental program can be switched on in the mature orchid flower, orchids provide an excellent system in which to study both the regulation of ovule development and the intercellular communication events that lead to the activation of this pathway. The Phalaenopsis orchid system is also amenable to biochemical investigations because ovule development is nearly synchronous, and thousands of ovules are present in each ovary, making tissue collection feasible.

The regulatory mechanisms that allow both the appropriate elaboration of the ovule developmental program and the biochemical specialization of differentiated cells involve the expression of appropriate genes in highly regulated patterns during development. Our group has chosen to assess the mechanisms involved in ovule development by identifying genes that are expressed uniquely in ovules, because these genes must play some role either in regulating development or in establishing the specialized identities of cells in the ovule. In this study, we isolated genes specific to developing and mature ovules of Phalaenopsis orchids by differential screening of cDNA libraries to explore the molecular basis of female gametophyte and ovule development. Using the unique developmental features of Phalaenopsis orchid ovules, we have identified several genes that are expressed at specific times and in specific cell types of the sporophyte tissue of the ovule and in the female gametophyte.

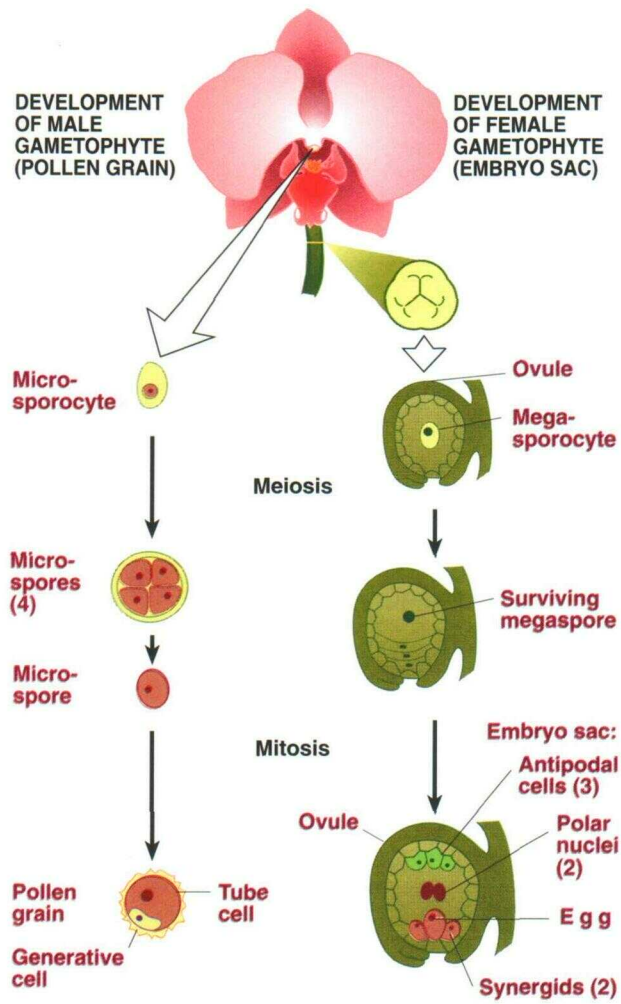

Figure 1. Diagram of Microgametogenesis and Megagametogenesis in Phalaenopsis.

Development of the male gametophyte (pollen grain) is completed before anthesis, whereas at anthesis the ovary is immature and lacks ovules. Pollination induces the ovule developmental program, resulting in the formation of a Polygonum-type female gametophyte.

RESULTS

Ovule Development in Orchids Is Induced by Pollination and Extends over 80 Days

Previously, our group presented a detailed account of Phalaenopsis ovule development and its regulation after pollination (Zhang and O'Neill, 1993). The major events during male and female gametophyte development in orchids are shown schematically in Figure 1. Although orchid flowers are unusual in that ovule development is delayed until anthesis of the flower and is triggered by pollination, once initiated, the processes of megasporogenesis and megagametogenesis are similar to those of many other plant species. The development of the mature female gametophyte is of the Polygonum type (Figure 1), which is found in 70% of all flowering plant species, including Arabidopsis, and is considered to be the prototypical program of female gametophyte development (Maheshwari, 1950; Bouman, 1984; Willemse and van Went, 1984; Reiser and Fischer, 1993).

We previously described in detail the regulation of female gametogenesis by pollination (Zhang and O'Neill, 1993). This study formed the basis of Figure 2, which illustrates the timeline of events in ovule development that spans ~80 days and provides the framework for consideration of the data presented in this study.

The first events in orchid ovule development are cell divisions within the meristematic region of the placental ridges that begin shortly after pollination. These ridges elongate and

branch dichotomously several times over the span of 4 weeks (Figure 2A). These branches form thousands of fingerlike ovule primordia at ~5.5 weeks after pollination (WAP). At this stage, cells in the epidermis and hypodermis are densely cytoplasmic. Next, a hypodermal cell near the apex of the primordia enlarges to form the archesporial cell. The inner integument initiates as a ring of periclinal cell divisions near the tip of the primordium, and the outer integument is initiated shortly thereafter (Figure 2B). This is accompanied by asymmetric growth and division of cells on one side of the primordium to establish the anatropous orientation of the ovule. Over the course of ~1 week, the archesporial cell enlarges further to form the megasporocyte directly (Figure 2C), which develops a distinctive polar distribution of organelles, enzyme activities, and callose within the wall. The nucellus remains uniseriate and is crushed between the inner integument and female gametophyte at maturity.

The megasporocyte undergoes meioses I and II to form the megaspores between 7 and 9 WAP. The micropylar megapores degenerate, and the chalazal megaspore enlarges as small vacuoles within it begin to coalesce. After the first division of the megaspore nucleus, the nuclei migrate to opposite ends of the coenocytic megagametophyte, where they divide twice to form the four chalazal and four micropylar nuclei of the eight-nucleate female gametophyte. The migration of a nucleus from each quartet to the center establishes the polar nuclei. The

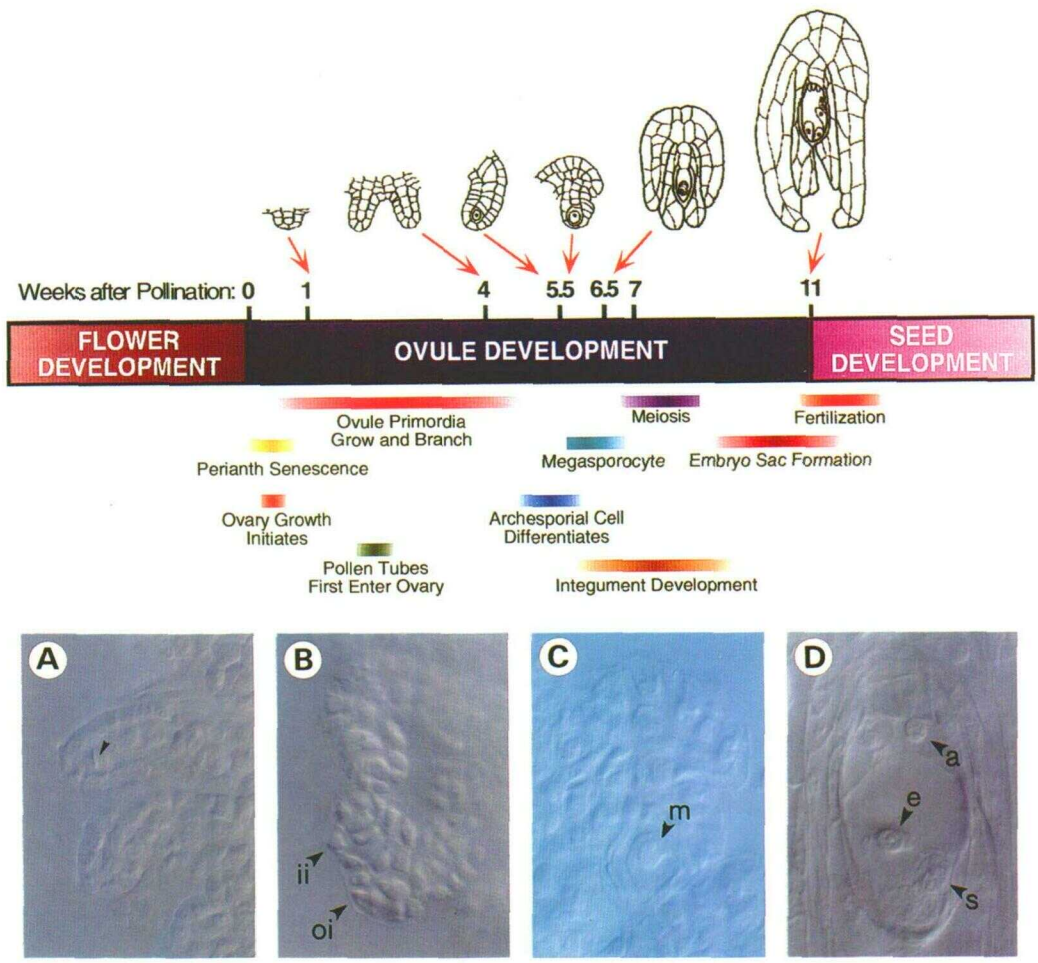

Figure 2. *Timeline of Phalaenopsis Ovule Development.*

The span of time during which each event takes place within a single ovary is indicated below the timeline. Ovules corresponding to four different stages of development were photographed using differential interference contrast microscopy.

(A) Meristematic protuberances. The inner cell file contains a cell undergoing a mitotic division (arrowhead).

(B) Ovule primordia with archesporial cells showing the beginnings of integument initiation. ii, inner integument; oi, outer integument.

(C) Ovule with megasporocyte and the inner integument surrounding one-half of the nucellus. m, megasporocyte.

(D) Ovule with mature female gametophyte. a, antipodal cell; e, egg cell; s, synergid.

three remaining nuclei at each pole become enclosed by cell walls to form three chalazal antipodal cells and two synergids and an egg cell at the micropylar pole. This results in the formation of a standard Polygonum-type female gametophyte (Maheshwari, 1950; Bouman, 1984; Willemse and van Went, 1984) over the course of ~2.5 weeks (Figure 2D). Ovules corresponding to each developmental time point in Figure 2 were isolated and used for the comparative analysis of gene expression at the level of mRNA populations.

Identification of cDNAs Expressed during Ovule Development

To identify transcripts that were expressed differentially during ovule development, cDNA libraries were constructed from mRNA isolated from Phalaenopsis orchid ovule tissue. Three pivotal events in the development of the female gametophyte were selected for this analysis, based on their obvious significance to the development of a fertile ovule and because they represent events that seemed most likely to involve significant changes in gene expression. These stages are shown in Figure 2. The first event targeted was the formation of the ovule primordia, as defined by fingerlike placental projections, each containing an archesporial cell (Figure 2B, early primordia library). Tissue corresponding to these stages was harvested at 5.5 WAP. The second event targeted was megasporocyte development and its transition to meiosis (Figure 2C, megasporocyte library). Ovule tissue representing this stage of development was harvested at 6.5 and 7.0 WAP, respectively, to include a range of late premeiotic and early meiotic events. Finally, development from the mitotic divisions in the four-nucleate stage through differentiation of the mature female gametophyte was placed in the third stage–specific library (Figure 2D, female gametophyte library). This cDNA library was constructed with ovule tissue harvarested at 11 WAP. We expected this library to contain transcripts involved in such processes as polar redistribution of organelles within the female gametophyte and differentiation of the cell types within the female gametophyte and sporophytic tissues of the ovule, in addition to transcripts involved in signaling between the female and male gametophytes.

The megasporocyte and female gametophyte libraries were selected for our initial screening efforts. These libraries were subjected to three-way differential screening, using cDNA probes reverse transcribed from ovary wall mRNA as control and ovule mRNA as experimental probes (6.5 and 11 WAP). This strategy allowed us to identify cDNA clones in each library that are characteristic of ovule tissue and to eliminate mRNAs shared with ovary tissue. Screening in this way provided information about the abundance of mRNAs in the ovule relative to the ovary wall in both libraries. Most genes related to photosynthesis and general housekeeping processes should be expressed in the ovary wall; therefore, clones selected by this strategy should represent genes that may not be unique to the ovule but are part of the contingent of genes responsible for the biochemical identity of cells in the ovule. This strategy also enabled us to make an initial observation of the stage specificity of the clones identified as more abundant in ovule tissue.

A total of 160 clones were selected based on their greater abundance in ovule tissue compared with ovary wall tissue at one or both stages examined, as well as 30 clones more abundant in ovary tissue. One-quarter of the clones more abundant in ovule tissue were chosen for further analysis and carried through secondary and tertiary screens. Restriction digestion analysis and cross-hybridization analysis of the resulting clones revealed a total of seven unique sequence classes, which were analyzed further.

Stage-Specific Expression of Ovule Genes

To determine the pattern of expression of these genes during ovule development and to confirm the differences in mRNA abundance observed in the screening process, each clone was used to probe RNA gel blots containing total RNA isolated from ovary or ovule tissue at various times after pollination, as shown in Figure 3. These time points correspond to stages of ovule

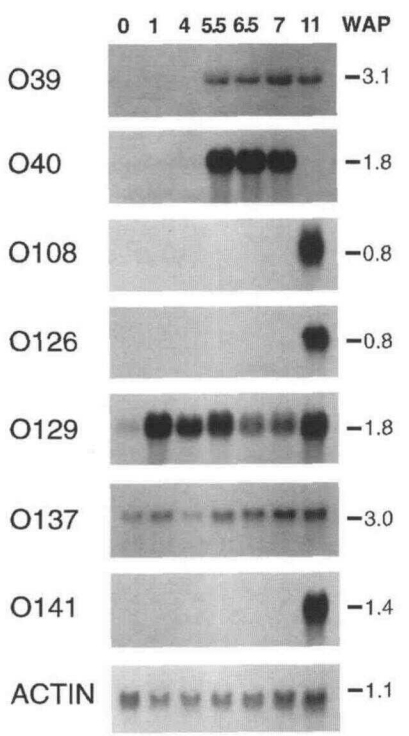

Figure 3. Stage-Specific Expression of Transcripts in Ovule Tissue.

RNA gel blot hybridization analysis of cDNAs corresponding to clones identified by differential screening was conducted. Numbers at the top represent times at which tissue was harvested in weeks after pollination. These numbers correspond to those shown in Figure 2, which illustrates the developmental events taking place at each time point. The clone name is indicated at left, and the clone length (in kb) is indicated at right. Actin served as a control. Twenty micrograms of total RNA was loaded per lane.

development described in the timeline of Phalaenopsis ovule development (Figure 2). In addition, all RNA blots were probed with a Phalaenopsis actin clone isolated by our laboratory to confirm the presence of undegraded RNA in each lane.

From this analysis, it was clear that the pattern of expression of the clones fell into three distinct classes. Two clones, O39 and O40, isolated from immature ovules at 6.5 WAP were expressed at high steady state levels at this developmental stage (Figure 3). Transcripts corresponding to both cDNAs were first detectable at 5.5 WAP, and the levels did not appear to change dramatically during development. O39 continued to be expressed up to the mature ovule stage, at 11 WAP. In contrast to O39, O40 expression was nearly absent by 11 WAP, but much longer autoradiographic exposure times (see Methods) revealed that O40 transcripts were faintly detectable at 4 and 11 WAP. The relative abundance of O40 transcripts was very high compared with that of O39, which required somewhat longer autoradiographic exposures. As can be seen from the timeline in Figure 2, these clones were expressed at high levels during stages when several key events were occurring, including integument initiation and growth, morphological differentiation of the megasporocyte, and subsequent entry into meiosis (5.5, 6.5, and 7.5 WAP). No ovule-specific clones isolated thus far were detected before 5.5 WAP, a time when ovule primordia are forming.

Several clones that were isolated from nearly mature ovules (O108, O126, and O141) fell into a second expression class. Transcripts corresponding to these clones were abundant at 11 WAP but were undetectable at early stages of development, even after long autoradiographic exposures. This time point represents the stage when most ovules are completing female gametophyte development and some ovules have been fertilized.

The remaining clones isolated from nearly mature ovules (O129 and O137) fell into a third expression class. Transcripts corresponding to these cDNAs were detected in ovule tissue at all stages but increased in abundance to reach a maximum at 11 WAP.

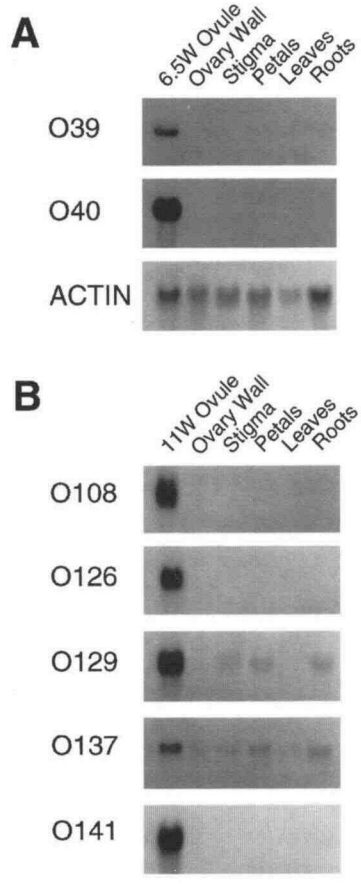

Figure 4. Tissue-Specific Expression of Ovule Clone Transcripts.

RNA gel blot hybridization analysis illustrates the abundance of transcripts corresponding to clones identified by differential screening in ovule, ovary wall, petal, stigma, leaf, and root tissues. Actin served as a control. Twenty micrograms of total RNA was loaded per lane.
(A) Transcripts detected early in ovule development. Ovule and ovary wall tissue was harvested at 6.5 WAP (6.5W).
(B) Transcripts detected late in ovule development. Ovule and ovary wall tissue was harvested at 11 WAP (11W).

Tissue-Specific Expression of Ovule Genes

Each clone was used to probe RNA blots containing total RNA isolated from various organs of the Phalaenopsis plant to determine whether the transcripts were present in other organs or were restricted to ovule tissues. Figure 4A demonstrates that mRNAs corresponding to clones O39 and O40 were not found in the ovary wall, in other floral organs such as the stigma or petals, or in other vegetative organs such as the leaves or roots. Figure 4B illustrates that O108 and O126 are specific to mature ovule tissues and are not detected in other tissues of the plant. Interestingly, O141 is present at high levels in ovules and is also detectable at low levels in roots. The remaining clones (O129 and O137) are present at quantitatively higher levels in ovule tissue, as would be expected from our screening strategy, but are also present in all organs of the plant examined.

Sequences Homologous to Ovule cDNAs Are Present in the Genome at Varying Abundance

To determine the approximate number of sequences in the Phalaenopsis genome homologous to each cDNA clone, we hybridized each clone to genomic DNA digested with EcoRI, BamHI, and HindIII at moderately high stringency (see Methods). Figure 5 shows that O39, O40, O126, and O141 are present as single-copy sequences. When the strongly hybridizing bands are considered, multiple fragments in each lane can be explained by restriction enzyme sites present in the cDNA. O40 shows fainter bands that may represent related sequences. In O108, O126, and O137, multiple bands of roughly equal intensity are present, indicating that these cDNAs are members of a small family of related sequences in the Phalaenopsis

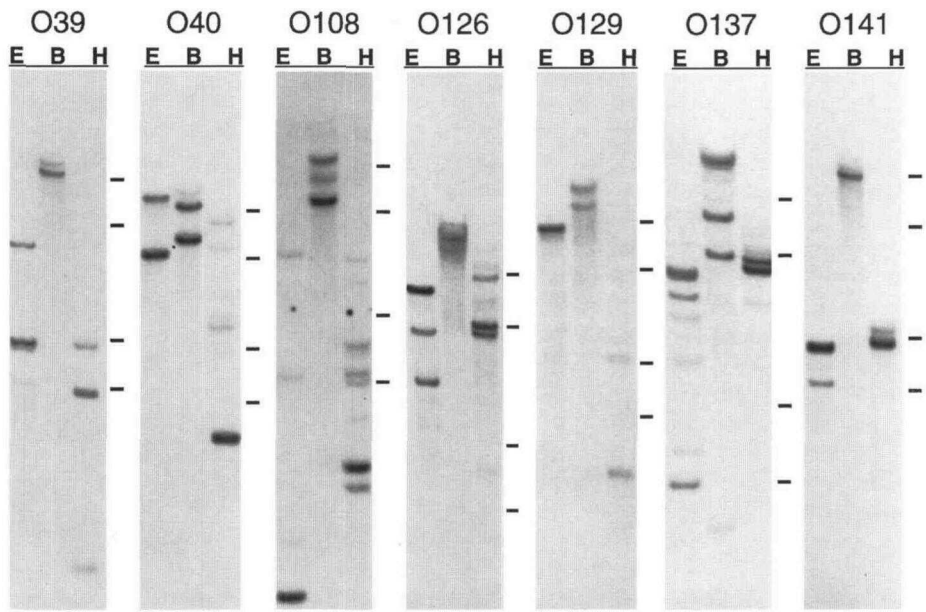

Figure 5. DNA Gel Blot Hybridization Analysis of Ovule cDNAs.

Each lane contains 10 μg of genomic DNA digested to completion with EcoRI (E), BamHI (B), or HindIII (H). The bars at the right of each blot indicate the position of markers corresponding to 12.0, 8.0, 4.0, and 3.0 kb, from top to bottom.

genome. In these cases, additional fainter bands are also apparent that may represent more divergent members of each gene family.

In Situ Hybridization Demonstrates That Some Ovule cDNAs Are Cell-Type Specific and That Some Are Expressed throughout the Ovule

In situ hybridization, using the cDNAs to probe tissue sections, was conducted to define precisely the spatial pattern of gene expression at different stages of ovule development. To attain the level of resolution necessary to identify specific cells within the ovule that express the gene of interest, we developed a technique that maintained the structural integrity of delicate tissues more completely than traditional paraffin-embedding techniques. To do this, we embedded all tissues in a UV light–polymerized methacrylate plastic mixture. This approach is a modification of a procedure that has been used for immunolocalization studies (Baskin et al., 1992) and has been described recently for in situ hybridization with RNA (Kronenberger et al., 1993).

039

Figure 6 illustrates the results of in situ hybridization conducted with O39 RNA probes to transverse sections through the orchid ovary under high-stringency conditions (see Methods). Figures 6A and 6B show that very little, if any, O39 transcript is present in the ovary at 3.5 WAP. In ovules at 3.5 WAP, the meristematic foci along the ridges have undergone several rounds of dichotomous branching and will branch at least once more to amplify the final number of projections available to form ovules. None of the projections in these sections have undergone the anatomical differentiation characteristic of the ovule primordia, such as the characteristically box-shaped cells in well-ordered files and an enlarged archesporial cell with a more diffusely staining nucleus. Figures 6A and 6B also illustrate the general observation that the hybridization signal was slightly more abundant over the tissue in sections of methacrylate-embedded tissue; however, this level of signal was equivalent to that observed in sections probed with the sense control strand (data not shown). This represents a low level of probe adherence to cell walls that is inherent in this procedure.

Figures 6C and 6D show that at the time of the archesporial cell differentiation in the ovule primordium, the intense hybridization signal is apparent primarily in the primordia themselves rather than in the subtending placental regions. Interestingly, some hybridization is also apparent in the unique layer of placental epidermal cells that appear dense and secretory and are located on the side of the placenta where pollen tubes grow. No hybridization was observed in the parenchymatous epidermal cells located on the opposite side of the placenta.

Hybridization with transcripts in the ovule tissue was observable, although at a lower level, throughout subsequent ovule development. Figures 6E and 6F illustrate ovules that show hybridization in all cells of the ovule, including the megasporo-

cyte. Ovules at this stage of development are undergoing rapid development of both integuments and have initiated the asymmetric growth that leads to the final anatropous orientation of the ovule. In Figure 6E, the megasporocyte of ovules has entered prophase I of meiosis. Very little hybridization is observed in the placental region of the ovary, with the exception of the placental epidermis.

Figures 6G and 6H illustrate ovules undergoing the final mitotic divisions of female gametophyte development. Once again, signal can be seen in all cells of the ovule, including the female gametophyte, although it is now more clumped in appearance. This is a direct result of the increased vacuolization of the ovule cells at this stage, which has pushed the cytoplasm to the cell corners where the signal is now localized. The layer of secretory cells on the outside of the placenta also showed hybridization with the O39 probe, although these tissues are not illustrated in Figures 6G and 6H.

These observations agree with those obtained by RNA gel blot hybridization analysis (Figure 3), which showed almost undetectable levels of O39 transcript in ovule tissue until 5.5 WAP, when transcripts were clearly detected. O39 continued to be expressed throughout ovule development and was still present at 11 WAP, when ovules are mature.

O40

Figure 7 shows in situ hybridizations with clone O40 to detect transcripts present in transverse sections of the orchid ovary. Contrary to our initial expectations based on RNA blot hybridization results, transcripts hybridizing to clone O40 are localized exclusively to the pollen tubes. The identification of this gene by our differential screening strategy was not completely unexpected, because pollen tubes become intertwined with the ovules in the ovary and consequently contribute to the RNA population harvested, despite our attempts to remove them (see Methods). The pollen tubes first enter the ovary at ~2 WAP (see Figure 2) and are present in the ovary until fertilization (Zhang and O'Neill, 1993).

Figures 7A and 7B illustrate tissue containing ovules at the archesporial stage of development, including many pollen tubes that were growing as a large mass in the locule adjacent to the specialized placental epidermis. Figures 7A and 7B show a very high level of O40 transcript present in the pollen tubes, compared with Figures 7C and 7D, which show sections from the same tissue block probed with the sense strand RNA as a control. No pollen tubes were present on the other side of the placenta, which does not differentiate specialized epidermal cells. In Figures 7A and 7B, the hybridization signal is localized primarily near the placenta rather than throughout the pollen tube mass; this observation is explained by the fact that the pollen tube tips, which contain the cytoplasm of the male gametophyte, track along the placental wall. This is illustrated by Figure 8B, which shows a longitudinal section of the ovary that has been stained with acridine orange and visualized with epifluorescence microscopy to show the location of RNA and DNA in the pollen tube. Clearly, the cytoplasm of the majority of pollen tubes in the area is localized near the placental surface, whereas the bulk of the tissue farther out in the locule is composed of empty pollen tubes left behind as the tips elongate. A higher magnification of the region in Figures 7A and 7B is presented in Figures 7E and 7F and shows ovule primordia, placenta, and pollen tubes in detail.

Later in ovule development, the pollen tubes become further intertwined in the ovules and continue to express the O40 transcript. Figures 7G and 7H illustrate pollen tubes growing on the placenta and the funiculus of ovules predominantly at the megasporocyte stage of development. Based on the integument length of the ovules shown in Figure 7G, some have already proceeded through meiosis. This is most likely the case for the ovule indicated by the arrowhead, which has a pollen tube that is expressing O40 transcript growing on its funiculus toward the ovule micropyle. The position of pollen tube tips at these later stages of ovule development can be observed more readily in Figure 8A, which illustrates the location of pollen tube cytoplasm (arrow) when surrounding ovules are mature. At this stage, pollen tubes are found predominantly on or very near the ovule funiculi.

Finally, Figures 7I and 7J illustrate mature ovules with pollen tubes that did not hybridize with the O40 probe. At this stage of ovule development, many ovules had been fertilized and pollen tubes may be growing less actively. This finding is consistent with RNA gel blot hybridization analysis, which shows dramatically reduced levels of O40 transcript in tissues harvested at 11 WAP (Figure 3), despite the fact that pollen tubes are undoubtedly still intertwined with the ovules during tissue collection.

O108

O108 transcripts could not be detected until 11 WAP, as expected from RNA gel blots. Figures 8C and 8D show that in mature ovules, O108 transcripts were present only in the outer layer of the outer integument and in the female gametophyte. In Figures 8C and 8D, each ovary section contains 20 to 50 randomly oriented ovules, which showed that the level of gene expression was variable among ovules in the same ovary. Many ovules did not express the gene at detectable levels, and these ovules were interspersed randomly with those that did. Examination of numerous sections did not reveal a discernible spatial pattern of organization of ovules within the ovary that might explain this observation, and ovules that expressed O108 were indistinguishable from those that did not at the anatomical level. This pattern of expression within the ovule population as a whole indicates that expression of O108 most likely occurs within a narrow developmental window; thus, small differences in stage between neighboring ovules result in the presence or absence of O108 transcripts.

Figures 8E and 8F illustrate a higher magnification view of numerous ovules containing O108 transcripts as well as showing several ovules that did not contain O108 transcripts. Figures 8E and 8F also demonstrate that O108 was not present in other tissues of the ovary, such as the hair cells that are derived

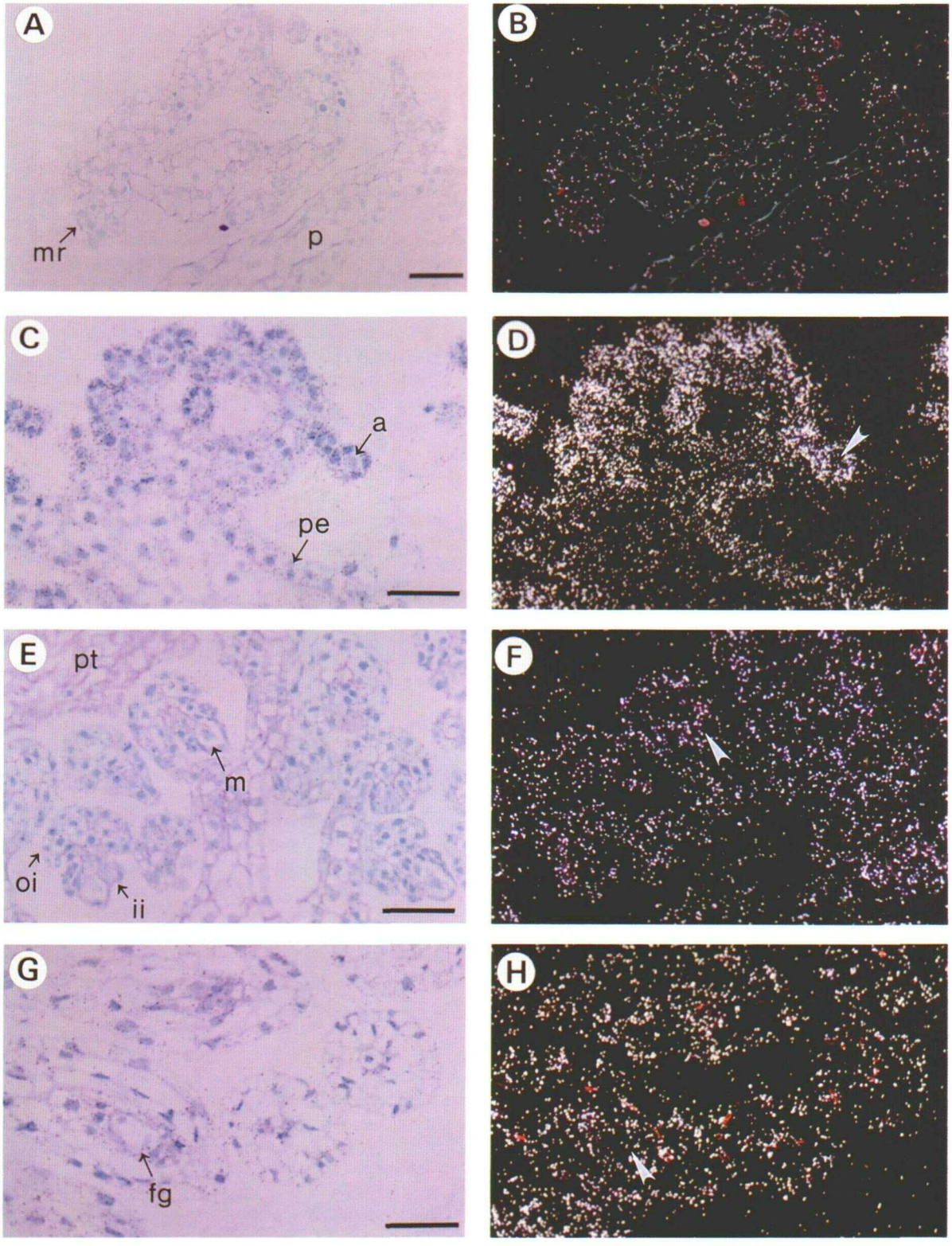

Figure 6. O39 RNA Distribution during Ovule Development.

from the inner ovary wall, or in the pollen tubes. In addition, background levels of hybridization with the placenta can be seen in Figures 8C and 8D, reinforcing data from RNA gel blot hybridization analysis that suggest that O108 gene expression is strictly ovule specific (Figure 4).

Some ovules express O108 in the integument but not in the central part of the ovule; this is illustrated by the ovules in transverse section in Figures 9A and 9B. In most of these cases, examination of serial sections led us to conclude that the plane of section did not pass through the female gametophyte but instead passed through sporophytic tissues in the center of the ovule. Figures 9C and 9D illustrate a section through the same ovules as shown in Figures 9A and 9B, but two of the ovules have been sectioned through the female gametophyte and thus show the centrally located O108 hybridization signal. No ovules expressed O108 in the female gametophyte but not in the integuments, although Figures 9C and 9D illustrate a rare example of an ovule in which O108 mRNA abundance is lower in the integument than in the female gametophyte. These observations allowed us to infer the temporal pattern of O108 gene expression. We conclude that O108 expression in the female gametophyte must coincide closely with expression in the outer integument.

Figures 9E to 9H illustrate longitudinal sections through ovules. In Figures 9E and 9F, O108 transcripts are localized to the outer cell layer of the outer integument and female gametophyte only, a point that can be seen most clearly at high magnification in Figure 9I. Furthermore, the funiculus does not express O108 mRNA. The ovule indicated by the arrowheads in Figures 9G and 9H was at the four-nucleate stage of female gametophyte development and did not show the signal, whereas the neighboring ovule had probably been fertilized recently and did show the signal. This reinforces the notion that O108 turns on during a narrow developmental window close to female gametophyte maturation and fertilization, as discussed earlier.

Occasionally, fertilized ovules were observed in sections that were recognizable due to the elongation of the outer integument relative to the inner integument (data not shown). The spatial pattern of cells that express the gene remains the same as that observed in prefertilization ovules, although the hybridization signal intensity was reduced and completely absent in some ovules at this stage. This suggests that the domain of expression of O108 does not shift during development and that expression of O108 is turned off or down-regulated after fertilization. The structural preservation of the postfertilization female gametophyte as well as the rudimentary nature of the orchid embryo (Wirth and Withner, 1959) prevented us from determining precisely when O108 expression decreases in relation to embryo development.

O141

In situ hybridization of immature ovules with clone O141 RNA probes showed no hybridization signal (data not shown), and the expression of this gene was restricted to the later stage of ovule development, as observed in RNA gel blot hybridization (Figure 3). Figures 10A and 10B indicate that hybridization with mature or nearly mature ovules occurred in both cell layers of the outer integument of the mature ovule rather than only in the outermost layer of the outer integument, as observed with clone O108. We observed no other tissues of the ovule that hybridized with O141 above background levels, even at very long exposures of several months. The O141 probe detected transcripts in only a subset of ovules in each section observed (Figures 10A and 10B). This is similar to the pattern observed for O108 and suggests that O141 was expressed only in a narrow window of time such that the slight differences in the developmental stage of neighboring ovules were reflected in O141 gene expression. In the case of O141, however, gene expression most likely began after fertilization. All of the ovules in which the gene was expressed showed the elongated outer integument characteristic of postfertilization ovules, as seen in Figures 10C and 10D. Higher magnifications of the ovule shown in Figures 10C and 10D (Figures 10E and 10F) showed a purple-staining pollen tube in the micropyle of the ovule (arrowhead). Furthermore, most ovules that expressed O141 mRNA had integuments that appeared slightly degraded in appearance, which accurately represented the condition of the ovules and was not a procedural artifact. At this stage, the outer integument had begun to develop into the seed coat, while the ovules progressed rapidly toward seed maturity.

Figures 10G and 10H illustrate once again that not all neighboring ovules were at precisely the same stage of development,

Figure 6. (continued).

Transverse sections through the placental region of the ovary were hybridized with antisense O39 RNA probes. Bright-field microscopy was used for **(A)**, **(C)**, **(E)**, and **(G)**; dark-field microscopy was used for **(B)**, **(D)**, **(F)**, and **(H)**. Some birefringence of the cell walls in methacrylate-embedded tissue can be observed in most sections and should not be confused with the true RNA hybridization signal, which is manifested as small white spots due to the presence of silver grains in the autoradiographic emulsion.

(A) and **(B)** Branching meristematic protuberances from the placenta. Bar = 50 μm.

(C) and **(D)** Archesporial-stage ovule primordia. The white arrowhead indicates an archesporial cell. Bar = 50 μm.

(E) and **(F)** Megasporocyte-stage ovules. The white arrowhead indicates a megasporocyte. Bar = 50 μm.

(G) and **(H)** Near-mature ovules. The white arrowhead indicates the female gametophyte. Bar = 50 μm.

a, archesporial cell; fg, female gametophyte; ii, inner integument; m, megasporocyte; mr, meristematic ridges; oi, outer integument; p, placenta; pe, placental epidermis; pt, pollen tubes.

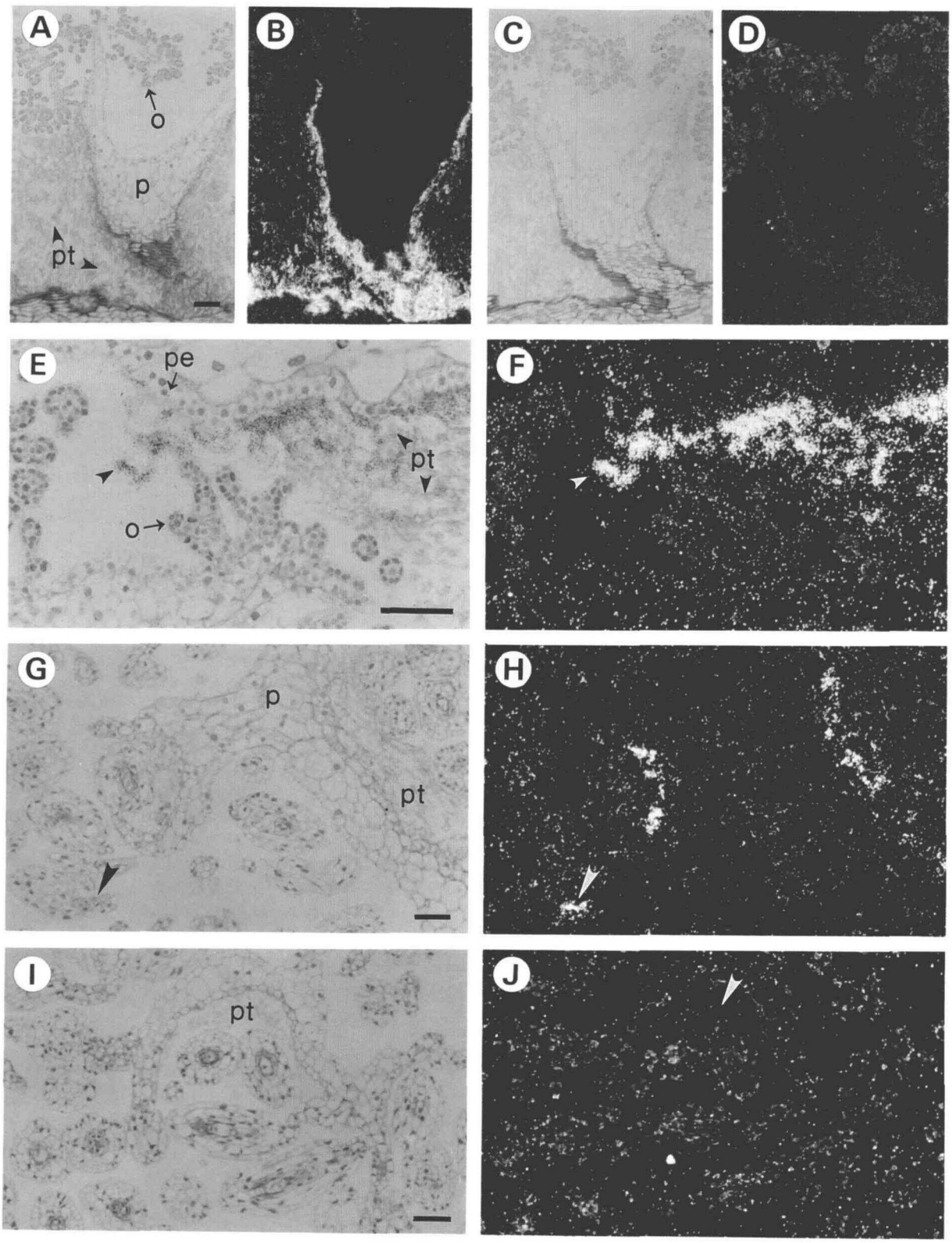

Figure 7. O40 RNA Distribution during Ovule Development.

based on gene expression pattern, despite their anatomical similarity. In addition, Figures 10G and 10H illustrate expression of O141 transcripts in isolated patches of placental epidermal cells. This was the only other location in the ovary in which O141 expression was observed during any stage of development.

Sequence Analysis of Ovule cDNAs Suggests That Some Are Involved in Gene Regulation Whereas Others Are Involved in Differentiation

Clone O39 Encodes a Homeobox Transcription Factor

Clone O39 represents an apparently full-length mRNA of 3088 nucleotides containing one long open reading frame (ORF) from position 298 to 2593, which is shown in Figure 11A. This ORF encodes a protein of 798 amino acids with a calculated molecular mass of ~84 kD and pI of 5.98. Sequence analysis indicated that a region near the N-terminal end of the protein exhibits strong similarity with the homeobox DNA binding motif of transcription factors. The archetypal homeobox consists of ~61 amino acids that form a helix-turn-helix structure capable of sequence-specific DNA binding (Scott et al., 1989). The predicted sequence of O39 retains all four of the absolutely conserved amino acids in the third recognition helix of the homeobox as well as nine of the 17 most highly conserved amino acids present throughout the homeobox; thus, it is likely to encode a true homeobox transcription factor (Figure 11B).

As with other homeobox protein families, O39 exhibits little sequence similarity to other homeobox protein families outside the homeobox region (Duboule, 1994). A notable exception is the recently identified GLABRA2 homeobox protein, which regulates trichome differentiation in Arabidopsis (Rerie et al., 1994). Amino acid sequence identity between O39 and GLABRA2 is 39% over the entire length of the protein and 66% within the homeobox region; overall structural organization is also similar between the two proteins, with the homeobox at the N-terminal end of the protein. In addition, O39 encodes a larger protein than most homeobox proteins, as does the *GLABRA2* gene (798 compared with 660 amino acids). When compared with other plant homeodomain proteins, the O39 homeodomain is most similar to Athb-1 and Athb-2 (HAT4 and HAT5) from Arabidopsis (Ruberti et al., 1991; Schena and Davis, 1992) and least similar to the maize protein KNOTTED1 (Vollbrecht et al., 1991). Figure 11B shows a multiple sequence alignment between O39 and other plant homeobox proteins compared with the consensus sequence for the plant homeobox proteins.

The cDNA also contains four short ORFs in the 5′ untranslated region (UTR) of the transcript, which are followed by stop codons (Figure 11A). The final three ORFs, which contain six, 19, and six codons, respectively, are in frame with the final and presumed coding region of the transcript. Although this structural feature has no known function in plants, short ORFs in the 5′ UTR of the yeast *GCN4* mRNA are involved in the translational control of expression of this transcription factor (Hinnebusch, 1990), and short ORFs have been observed in the 5′ UTR of several plant homeobox genes (Ruberti et al., 1991; Bellmann and Werr, 1992; Schindler et al., 1993) and in the transcripts of several other types of gene regulatory proteins in plants (Hartings et al., 1989; Singh et al., 1990).

Clone O40 Encodes a Cytochrome P450 Mixed Function Monooxygenase

Sequence analysis of clone O40 indicated that the largest ORF encodes a cytochrome P450 monooxygenase with a predicted molecular mass of 48 kD and a pI of 6.62. The cytochrome P450 monooxygenases are a large superfamily of membrane-bound enzymes that catalyze the oxidation of diverse and often overlapping substrates of both endogenous and xenobiotic origin in organisms from bacteria to fungi, plants, and animals (Nebert and Gonzalez, 1987; Donaldson and Luster, 1991). These enzymes employ a heme group linked to the polypeptide through a cysteine residue in the motif FxxGxxxCxxG (where x is a nonconserved amino acid) that is present in all cytochrome P450 monooxygenases. Catalytic activity is accomplished by complexing the substrate with the heme moiety, which then acts to transfer an electron from the donor NADPH reductase to molecular oxygen, resulting in the reduction of molecular oxygen to H_2O and the oxidation of the substrate (Goodwin and Mercer, 1988).

The complexity of evolutionary relationships between the

Figure 7. (continued).

Sections through the placental region of the ovary were hybridized with sense and antisense O40 RNA probes. Bright-field microscopy was used for **(A)**, **(C)**, **(E)**, **(G)**, and **(I)**; dark-field microscopy was used for **(B)**, **(D)**, **(F)**, **(H)**, and **(J)**.

(A) and **(B)** Low-magnification view of archesporial-stage ovule primordia and placenta with pollen tubes in the locule. Hundreds of pink-staining pollen tubes are present in the locule. Bar = 100 μm.

(C) and **(D)** Same tissue as shown in **(A)** and **(B)** hybridized with the sense RNA probe as a control. Bar in **(A)** = 100 μm for **(C)** and **(D)**.

(E) and **(F)** Higher magnification of the section shown in **(A)** and **(B)** showing pollen tubes growing along the placental epidermis with archesporial-stage ovule primordia. The arrowheads in **(E)** and **(F)** indicate a pollen tube tip. Bar = 50 μm.

(G) and **(H)** Ovules at the megasporocyte stage or slightly later stages with pollen tubes. The arrowheads in **(G)** and **(H)** indicate a pollen tube growing on the funiculus of an ovule. Bar = 50 μm.

(I) and **(J)** Mature ovules with pollen tubes that do not express O40. The white arrowhead in **(J)** indicates an area filled with pollen tubes. Bar = 50 μm.

o, ovule primordium; p, placenta; pe, placental epidermis; pt, pollen tubes.

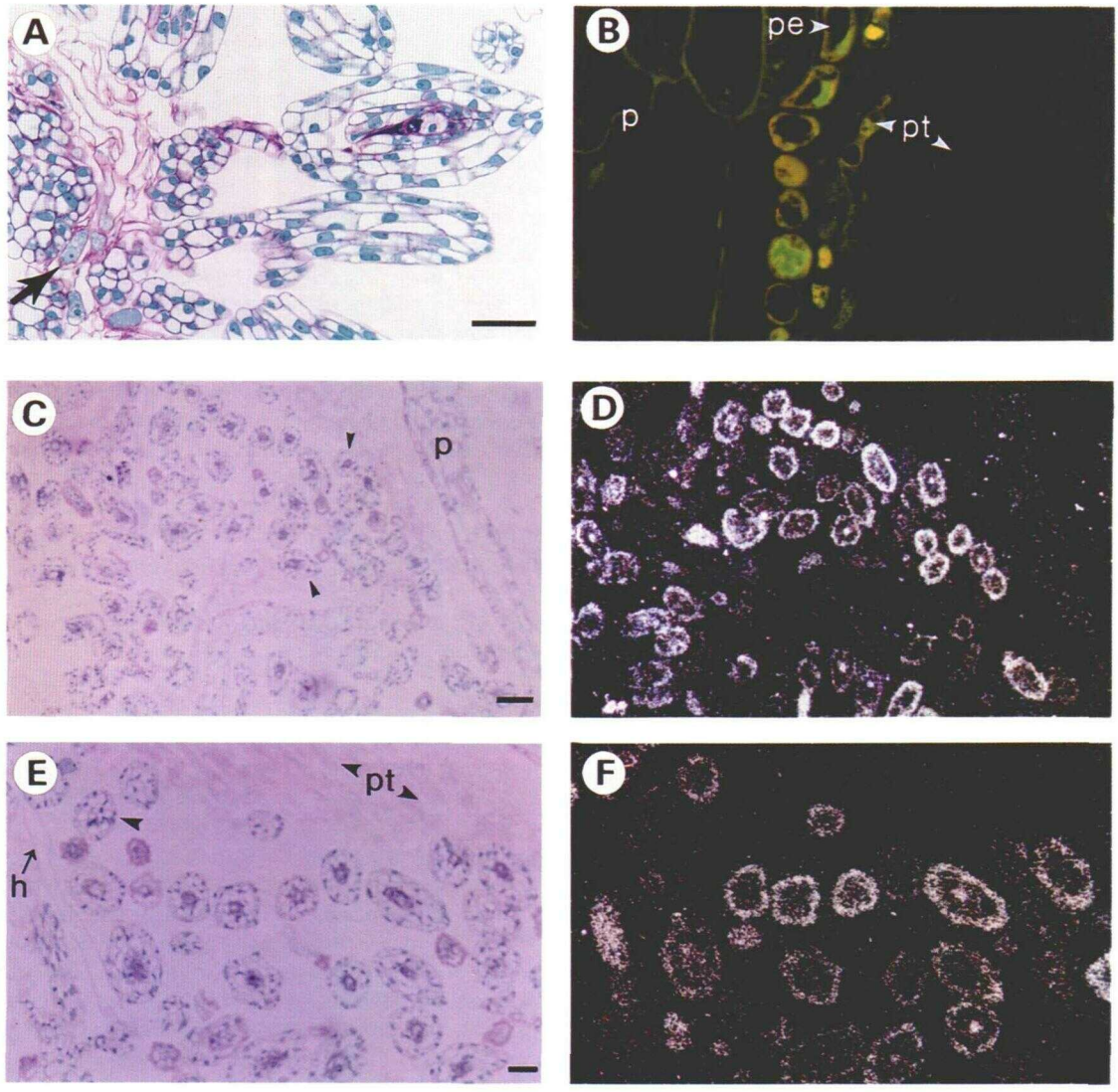

Figure 8. Pollen Tubes in the Ovary and O108 RNA Distribution during Ovule Development.

Sections through the placental region of the ovary were hybridized with O108 RNA probes. Bright-field microscopy was used for **(C)** and **(E)**; dark-field microscopy was used for **(D)** and **(F)**. The arrowheads indicate ovules that do not express O108.

(A) Bright-field microscopy of mature and fertilized ovules with pollen tubes intertwined. Pollen tube cytoplasm is localized to the tip (arrow). Bar = 50 μm.

(B) Longitudinal section of the inner ovary wall stained with acridine orange and visualized with epifluorescence microscopy.

(C) and **(D)** Mature ovules showing expression of O108. Bar = 100 μm.

(E) and **(F)** Higher magnification view of the ovules shown in **(C)** and **(D)**. Bar = 50 μm.

h, hair cell; p, placenta; pe, placental epidermis; pt, pollen tubes.

families of cytochrome P450 monooxygenases has led to the arbitrary convention that sequences exhibiting ⩽40% amino acid identity are considered to be members of different gene families and sequences within a family are considered to be members of the same gene subfamily if they share ⩾68% similarity (Nebert and Gonzalez, 1987). By this convention, O40 represents the second member of the CYP78 gene family and consequently has been named CYP78A2 by the Cytochrome P450 Gene Nomenclature Committee (Nelson et al., 1993).

Figure 12 illustrates the relationship between O40 and other plant cytochrome P450 monooxygenases. The amino acid sequence of O40 is most similar to the maize tassel cDNA 1

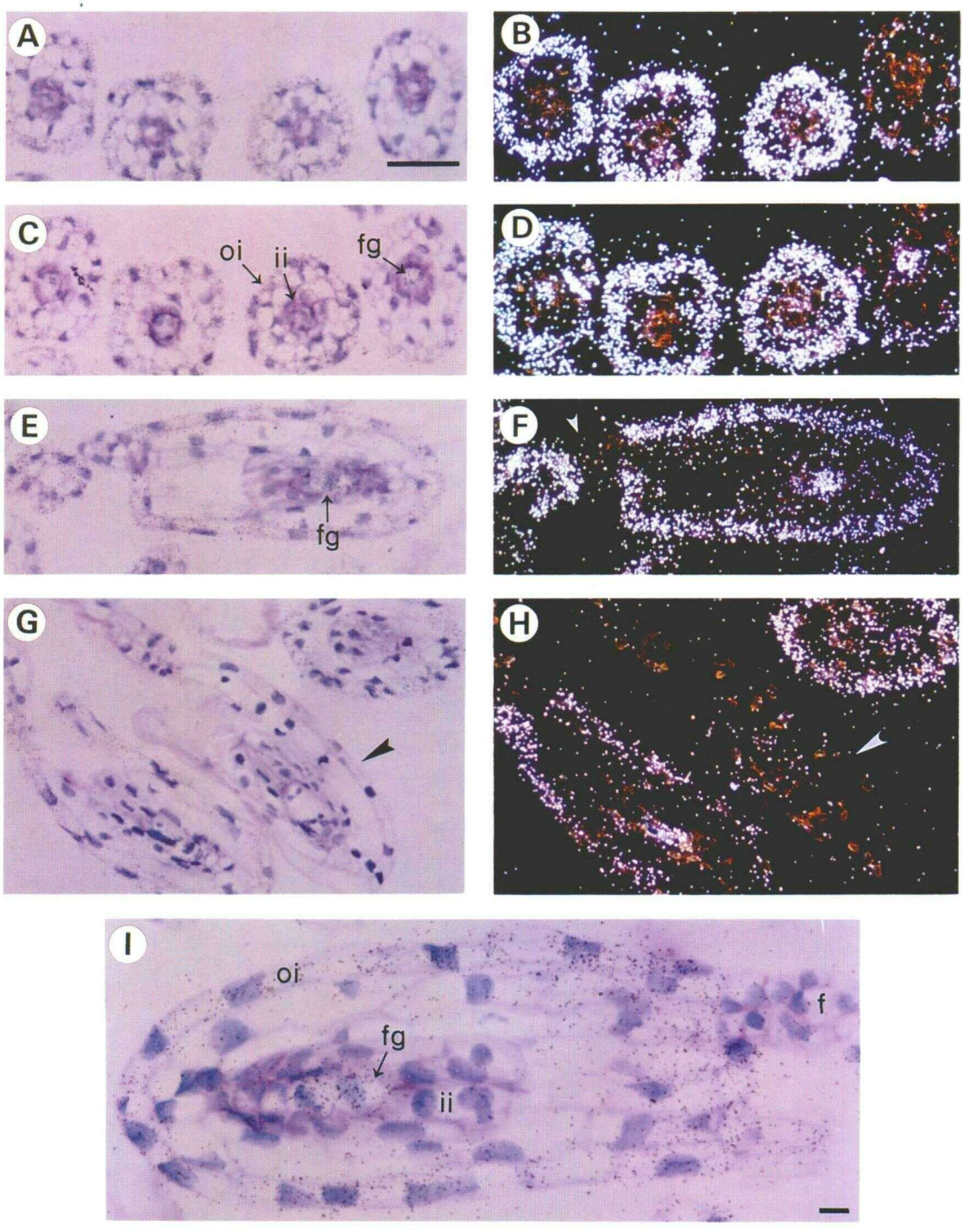

Figure 9. O108 RNA Distribution in Mature Ovules.

Sections through the placental region of the ovary were hybridized with antisense O108 RNA probes. Bright-field microscopy was used for **(A)**, **(C)**, **(E)**, **(G)**, and **(I)**; dark-field microscopy was used for **(B)**, **(D)**, **(F)**, and **(H)**.

(A) and **(B)** Transverse sections of mature ovules showing expression of O108. Bar = 50 μm.

(C) and **(D)** Serial section of the same ovules shown in **(A)** and **(B)**.

(E) and **(F)** Longitudinal section of a mature ovule. White arrowhead indicates the funiculus.

(G) and **(H)** Longitudinal section of two ovules (arrowheads), one mature and one at the four-nucleate stage of female gametophyte development.

(I) Mature ovule showing hybridization signal in the outer layer of the outer integument and the female gametophyte. Bar = 10 μm.

f, funiculus; fg, female gametophyte; ii, inner integument; oi, outer integument.

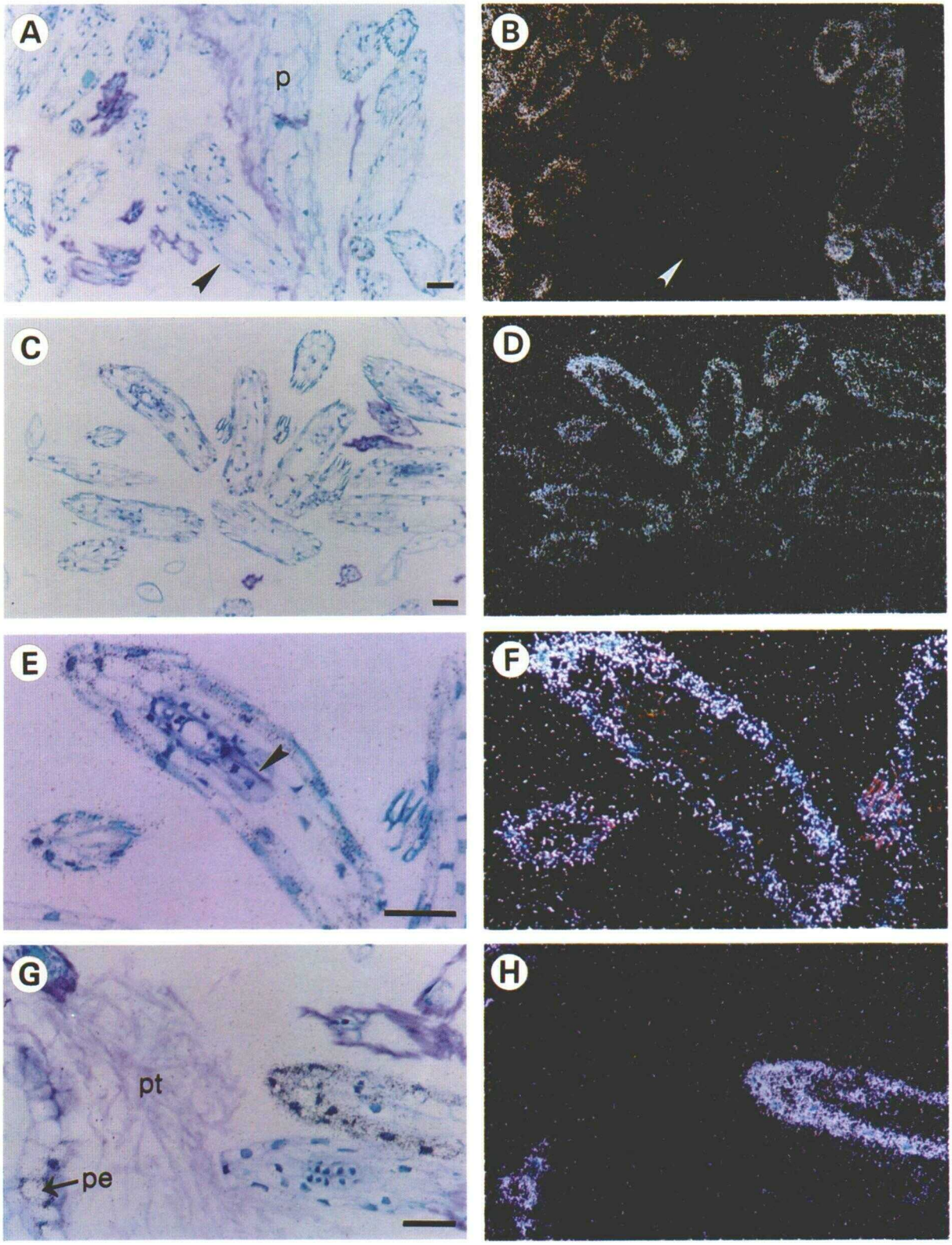

Figure 10. O141 RNA Distribution in Mature Ovules.

(MTC1; CYP78A1), with which it shows 54% amino acid identity (Larkin, 1994). O40 also shares sequence similarity with several other recently identified plant cytochrome P450 monooxygenases, including 35% amino acid identity with CYP71A1 from avocado, which increases in abundance in the pericarp during ripening (Bozak et al., 1990). When compared with a number of other plant cytochrome P450 monooxygenases, O40 exhibits 35% identity with flavonoid-3′, 5′-hydroxylase (CYP75A3) from petunia (Holton et al., 1993) and 29% identity with cinnamate 4-hydroxylase (CYP73A1) from Jerusalem artichoke (Teutsch et al., 1993) and with cinnamate 4-hydroxylase (CYP73A2) from mung bean (Mizutani et al., 1993).

Clone O108 Encodes a Novel Peptide of Unknown Function

Clone O108 contains several ORFs, and the longest one encodes a putative protein product of ~15 kD with a predicted pI of 5.37, illustrated by Figure 13. Comparison of the sequence of this clone with the data base of known sequences revealed no obvious similarity with genes of known function but showed significant similarity with an expressed sequence tag (EST) from Arabidopsis. To glean more information about the two clones through comparison of the deduced protein sequences, the 629-bp Arabidopsis EST clone also was sequenced fully (data not shown). The most similarity between the two clones lies in the 5′ region of the mRNA, upstream of the first methionine codon in O108 (data not shown), which leads us to believe that the orchid clone may not be full length. O108 lacks only a few nucleotides, however, because the 783-bp cDNA corresponds closely to the length of the transcript observed by RNA gel blot hybridization analysis (Figure 3). Similarity between the Arabidopsis and Phalaenopsis sequences is highest in the N-terminal and C-terminal regions but lower in the middle of the predicted peptides (data not shown). The putative protein encoded by O108 contains a consensus ATP/GTP binding site at the C-terminal end (Figure 13), a characteristic shared by the predicted peptide encoded by the EST clone.

Clone O126 Encodes a Glycine-Rich Protein

Clone O126 is 867 bp in length, as shown in Figure 14. The most reasonable ORF encodes an ~18-kD protein rich in glycine residues, with a predicted pI of 3.71. The cDNA is probably not full length, although as with O108, it corresponds closely to the transcript length as determined by RNA blot hybridization (Figure 3). The putative protein contains a probable signal peptide sequence (von Heijne, 1986), minus several residues of the signal peptide and the initial methionine, making it likely that the protein is secreted to the cell wall. Overall, the putative protein is 31% glycine and is 42% glycine within the glycine-rich region from residue 45 to 190. This falls well within the range for glycine-rich proteins that are thought to be structural components of the plant cell wall. Moreover, as in other cell wall glycine-rich proteins, O126 contains a slightly irregular repeated sequence motif that is found four times. The protein does not, on the other hand, contain the consensus ribonucleotide binding domain found in several plant glycine-rich proteins that appear to be localized to the cytoplasm, nor does it show similarity with heterogeneous nuclear ribonuclear protein A1.

These characteristics led us to believe that O126 is a cell wall structural protein similar to those isolated from a variety of monocot and dicot species, including *Phaseolus vulgaris* (Keller et al., 1988), petunia (Condit and Meagher, 1986; Linthorst et al., 1990), Arabidopsis (de Oliveira et al., 1990, 1993; Quigley et al., 1991), *Nicotiana sylvestris* (Obokata et al., 1991), tomato (Showalter et al., 1991), soybean (Sandal et al., 1992), barley (Rohde et al., 1990), and rice (Fang et al., 1991; Lei and Wu, 1991). Significant sequence similarity in the higher order repeats or in the residues interspersed with glycine residues has not been observed between O126 and other reported sequences, however, suggesting that O126 encodes a novel glycine-rich protein, which we have named PGRP-1. The glycine-rich domain of the protein is highly acidic, containing 10% aspartate and 3.5% glutamate, in contrast to the majority of reported glycine-rich proteins, which are either hydrophobic or basic in nature.

Clone O141 Is Homologous to Cysteine Proteinases

Sequence analysis of clone O141 revealed that the 1347-bp cDNA encodes a putative protein of ~40 kD and predicted pI of 6.36, as shown in Figure 15. The length of the cDNA is slightly shorter than the 1.4-kb mRNA observed by RNA gel blot hybridization, so the ORF most likely begins at position 12 of the cDNA. The predicted polypeptide is most similar to endopeptidases from *Vigna mungo*, *P. vulgaris*, *Vicia sativa*, and soybean, with which it shares 67, 66, 64, and 60% overall identity, respectively (Mitsuhashi and Minamikawa, 1989; Kalinski

Figure 10. (continued).

Sections through the placental region of the ovary were hybridized with antisense O141 RNA probes. Bright-field microscopy was used for **(A)**, **(C)**, **(E)**, and **(G)**; dark-field microscopy was used for **(B)**, **(D)**, **(F)**, and **(H)**.

(A) and **(B)** Fertilized ovules and placenta. One mature but fertilized ovule does not show hybridization (arrowheads). Bar = 50 μm.

(C) and **(D)** Mature ovules showing the hybridization signal. Bar = 50 μm.

(E) and **(F)** Higher magnification of one ovule as shown in **(C)** and **(D)** with a pollen tube in the micropyle (arrowhead in **[E]**). Bar = 50 μm.

(G) and **(H)** Two adjacent ovules with varying patterns of gene expression. Also shown are several cells of the placental epidermis with hybridization signal. Bar = 50 μm.

p, placenta; pe, placental epidermis; pt, pollen tubes.

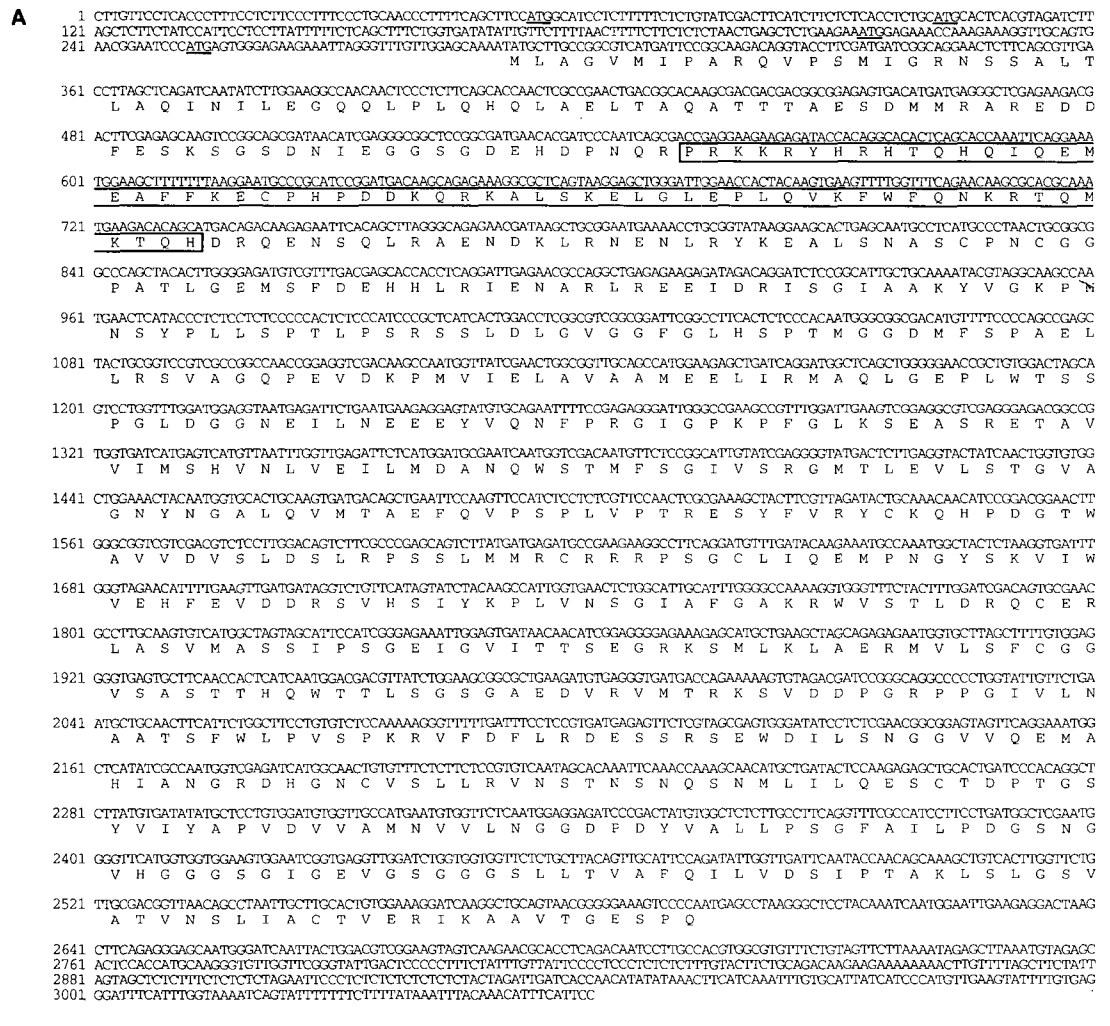

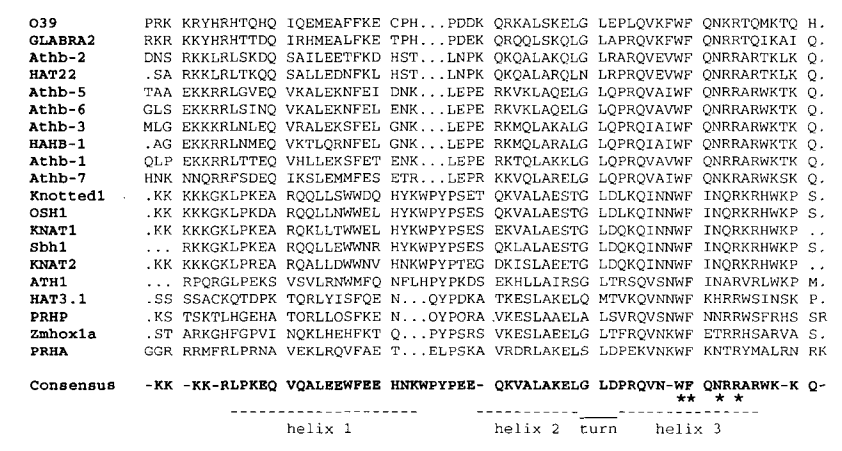

Figure 11. Sequence Analysis of Clone O39.

(A) Nucleotide and deduced amino acid sequences of clone O39. The homeodomain is boxed, and start codons upstream of the coding sequence are underlined. The GenBank accession number of this sequence is U34743.

(B) Amino acid sequence alignment of the homeodomain regions of O39 with other plant homeodomain proteins. The most invariant residues in helix 3 of the homeodomain are indicated by asterisks. The GenBank accession numbers corresponding to other plant nucleotide sequences encoding these proteins are as follows: *GLABRA2*, L32873; *HAT22*, M90417; *HAT3.1*, X69512; *Athb-1*, X58821; *Athb-2*, X68145; *Athb-3*, X62644; *Athb-5*, X67033; *Athb-6*, X67034; *Athb-7*, X67032; *ATH1*, X80126; *KNAT1*, U14174; *KNAT2*, U14175; *PRHA*, L21991; *PRHP*, L21975; *Sbh1*, L13663; *Knotted1*, X61308; *OSH1*, D16507; *Zmhox1a*, X67561; *HAHB1*, L22847.

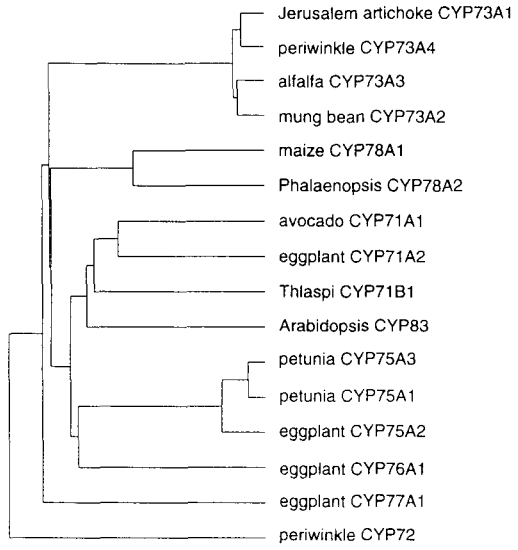

Figure 12. Dendrogram Illustrating the Sequence Relationship between O40 and Other Plant Cytochrome P450 Monooxygenases.

The GenBank accession number of O40 (Phalaenopsis CYP78A2) is U34744. The GenBank numbers corresponding to the other sequences are as follows: maize CYP78A1, L23209; Arabidopsis CYP83, U18929; petunia CYP75A1 and CYP75A3, Z22545 and Z22544, respectively; avocado CYP71A1, M32885; eggplant CYP71A2, CYP75A2, CYP76A1, and CYP77A1, D14990, X70824, X71658, and X71656, respectively; periwinkle CYP72 and CYP73A4, L19074 and Z32563, respectively; *Thlaspi arvense* (Thlaspi) CYP71B1, L24438; Jerusalem artichoke CYP73A1, Z17369; mung bean CYP73A2, L07634; alfalfa CYP73A3, L11046.

et al., 1990; Tanaka et al., 1991). The predicted polypeptide also shares significant identity with the well-characterized fruit endopeptidases papain (43%) and actinidin (45%) as well as with the aleurone-specific endopeptidase aleurain (39%) (Rogers et al., 1985; Cohen et al., 1986; Praekelt et al., 1988). It is likely that O141 encodes an authentic endopeptidase enzyme because it contains the consensus sequences surrounding the three key amino acids critical to catalysis (Cys-155, His-290, and Asn-311 of O141) and nine of 10 type II glycine residues found in both papain and actinidin that are important to the overall protein conformation (Kamphuis et al., 1985).

Examination of the predicted amino acid sequence suggests that the first 19 residues represent a signal sequence that is cotranslationally removed from the protein to yield a 38-kD product (von Heijne, 1986). Alignment of the O141 sequence with the mature peptides of other cysteine proteinases suggests that it may be processed to produce a mature 25-kD protein in a manner similar to that of other cysteine proteinases, most likely by proteolytic cleavage before the leucine in position 131. There is evidence that removal of the prosequences of both papain and the *V. mungo* cotyledon enzyme results in activation of the enzyme. The similarity between O141 and these proteins suggests that it also may undergo conversion to an active peptide, thus possibly providing a mechanism to limit enzyme activity to the appropriate cellular compartment or developmental milieu. Interestingly, both O141 and the cysteine proteinases to which it is most similar contain endoplasmic reticulum retention signals at the C-terminal end (Denecke et al., 1992), suggesting that they might usually function in this cellular compartment. O141 does not contain potential glycosylation sites in the mature peptide or prosequences of the peptide, unlike several similar proteinases that are thought to be transported through the secretory pathway.

DISCUSSION

There is ample evidence from various sources, for example, from solution hybridization experiments (Kamalay and Goldberg, 1980, 1984) and genetics (Meyerowitz and Somerville, 1994), that the highly precise pattern of development and tissue differentiation in plant organs results from the expression of specific subsets of genes in defined temporal and spatial domains. For this reason, we have used the Phalaenopsis orchid as a model system to identify genes expressed predominantly in ovules, because these genes are involved in the regulation of development or in the differentiation of cell types within the ovule. Using a differential screening approach, we identified a number of transcripts that increase in abundance during specific stages of ovule development. We also identified one transcript that is expressed solely in pollen tubes. The ovule-specific genes can be placed into three basic classes, based on their pattern of expression. Several genes identified (O129 and O137) become more abundant in

```
  1 AATTCGGCACGAGTATGAAAGGAGAAAGGTGACTTTGAAGAGCTCGGCGAAGAATTCTTG
 61 GTAGAAGAAGCCGTGGCAATGGAGTCTCGGATGATCCGTTACATGATTTGGGATGGACTA
                    M  E  S  R  M  I  R  Y  M  I  W  D  G  L

121 GCAGGTGACGTGATTGAACTCCCTGGCGTGAAGGGTAAGTTTCTATCTATGATTCTTGAT
    A  G  D  V  I  E  L  P  G  V  K  G  K  F  L  S  M  I  L  D

181 TTTTGCAAGAAACGTGTTGCATGGGCTGCTGGCGGCGATGGGACGTTGGAAGGCTTGAAA
    F  C  K  K  R  V  A  W  A  A  G  G  D  G  T  L  E  G  L  K

241 TCTGATTTTGTGAATGTTGATTTGGGCACACTGATCCATCTTGGTGCAGCAAGCTTTTAT
    S  D  F  V  N  V  D  L  G  T  L  I  H  L  G  A  A  S  F  Y

301 CTGAAAACAAATGATTTGGTTGATTTGACCTCTCAAACTTTAGCAAATCGGATTCAGGGG
    L  K  T  N  D  L  V  D  L  T  S  Q  T  L [A  N  R  I  Q  G

361 AAGACTATTGAAGAGGTTTGCAGGGCCTTGAACCCTGAAGAATAAAAGGAGATTCAGATG
    K  T] I  E  E  V  C  R  A  L  N  P  E  E

421 GAGAATTCGTGGACATTTGAGTGAAATGATGGTGGTGCTCTCTCTCTCTCCCCCCACA
481 CCTTCGCCCTATATTTACTATGAGTCTCTTTAGTTTCTATTTTATTTGATCATGTTGAG
541 TCTAGTGTGTTCTCTATACTTATTTGAAAGTGATGATTGTCTTTTATTTGCTGTTGCAAG
601 TTTAGGGTAAGAAAGTTGAAATAACATAACATATGTATCTCTCGAAACACTTTTGGTGCC
661 AACTTAAAGCTACCATCTATATAATTTTGACACTTGTGTATTAATATCGTTGGGTCCTTT
721 CAACAACTTGTGTTTAGCTATGTAATTTCGCTATTTGTGTTTACATATTACATCTATTTT
781 CT
```

Figure 13. Nucleotide and Deduced Amino Acid Sequence of Clone O108.

Amino acids of the consensus ATP/GTP binding site are boxed. The GenBank accession number of this sequence is U34745.

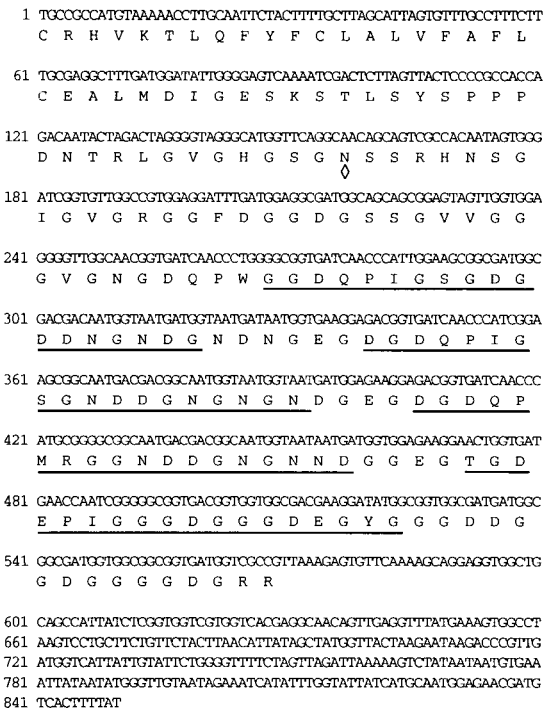

Figure 14. Nucleotide and Deduced Amino Acid Sequence of Clone O126.

Irregular repeats in the amino acid sequence are underlined, and a potential N-glycosylation site is indicated by an open diamond. The GenBank accession number of this sequence is U34746.

the mature ovule but are expressed at all stages of ovule development and in all tissues of the plant. Another class, represented by clone O39, begins to be expressed during early development and is expressed almost exclusively in the ovule. The third class of genes, represented by clones O108, O126, and O141, is expressed almost exclusively in maturing ovules.

As has been observed in studies of male reproductive development (Stinson et al., 1987; Ursin et al., 1989; Koltunow et al., 1990), examination of the spatial pattern of gene expression studied here suggests that complex developmental programs are active within the ovule that lead to diverse domains of gene expression. The isolation of ovule-specific genes now provides the tools for examining both the regulatory mechanisms involved in controlling gene expression and the function of genes expressed in specific domains during ovule development.

Early Development

O39 Homeobox Protein

One of the best characterized classes of transcription factors known to regulate developmental decisions is the homeobox

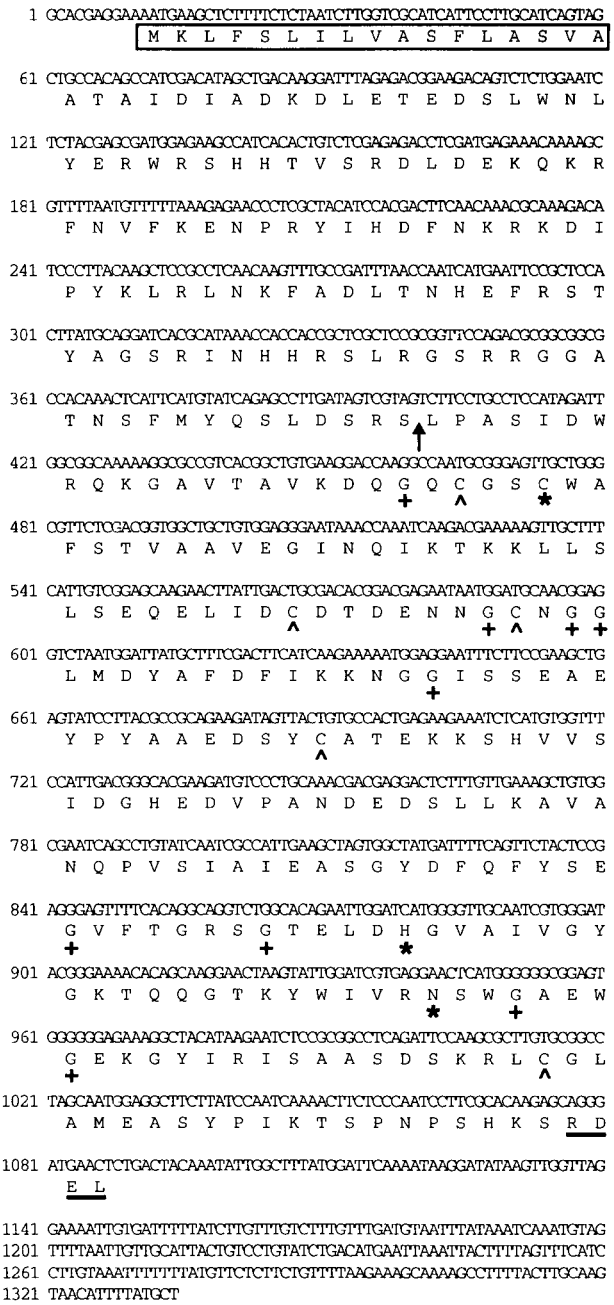

Figure 15. Nucleotide and Deduced Amino Acid Sequence of Clone O141.

Residues of the active site are indicated by (*), probable type II glycines that contribute to protein tertiary structure are indicated by (+), cysteines that may form disulfide linkages are indicated by (^), the potential propeptide cleavage site is indicated by an arrow, the endoplasmic reticulum retention signal is underlined, and the predicted signal peptide is boxed. The GenBank accession number of the O141 sequence is U34747.

protein. Homeobox proteins bind DNA in a sequence-specific manner to regulate the expression of target genes during development (Scott et al., 1989; Gehring, 1993). The activity of downstream target genes leads ultimately to the biochemical specialization of cells in patterns determined by the expression of the master regulatory homeobox protein. This activity is exemplified by the homeotic mutants in Drosophila that transform segments of the body plan into a segment that would normally form elsewhere, for example, as a result of mutations in homeobox genes (Lawrence and Morata, 1994). In animal systems, large numbers of homeobox proteins that play various roles in gene regulatory cascades during development and differentiation have been identified (see Duboule, 1994, for a listing of homeobox gene classes). Typically, homeobox proteins are divergent outside the region of the homeobox. These regions are thought to allow for interactions with other protein partners in order to yield variation in binding site affinities and cellular activities, which helps to explain the diverse developmental roles played by these proteins.

Recently, a number of homeobox genes have been isolated from plants, including the *Knotted1*-like genes that appear to play a role in maintaining the indeterminacy of plant cells (Vollbrecht et al., 1991; Jackson et al., 1994). Other plant homeobox proteins may play a role in activating genes involved in the host response to pathogen infection (PRHP and PRHA) (Korfhage et al., 1994) and, as most recently discovered, in the appropriate differentiation of the Arabidopsis trichome (*GLABRA2*) (Rerie et al., 1994). Thus, it is likely that clone O39, which contains a homeodomain, plays a role in gene regulation during ovule development.

Recent investigations of the *Mgr3* and *Mgr9* mutants of tobacco have led to conclusions that may assist in understanding the role of the O39 gene product in ovule development. Examination of the behavior of the ovules of both normal and mutant plants in tissue culture provided evidence that tobacco ovule primordia become committed to develop as ovules shortly before the formation of the nucellus and the initiation of the ovular integuments (Evans and Malmberg, 1989). Extending these observations to the time course of ovule development in Phalaenopsis, it is possible that the commitment to ovule development occurs between 4 and 5.5 WAP (Figure 2), when ovule primordia with recognizable archesporial cells are first apparent. This corresponds with the time when O39 begins to be expressed (Figures 3, 6C, and 6D). In situ hybridization analysis demonstrated that the O39 transcript is present throughout the ovule primordium at early stages as well as throughout the various differentiating ovule tissues at later stages of development (Figures 6D to 6G). The specificity of this transcript to ovule tissue, the timing of its expression, and the broad domain of expression in all cells of the ovule led us to hypothesize that this putative transcription factor may play a role in initiating the program of ovule development. Alternatively, it is possible that O39 expression is induced in response to the commitment to ovule differentiation and that its gene product acts to regulate a subset of genes involved in the developmental pathway.

It is intriguing that expression of O39 continues through the stage at which the ovule is mature and receptive to fertilization and that in situ hybridization experiments show that the transcript continues to be expressed throughout the ovule, even at late stages of development, when meristematic cell layers have differentiated into diverse tissues (Figures 6D to 6H). It is possible that the cells of the ovule require the presence of the homeodomain protein to continue appropriate differentiation. Just such a requirement has been described for Drosophila adult epidermal cells, which require the continuous expression of homeotic selector genes to attain the appropriate fate (Castelli-Gair et al., 1994). On the other hand, other tissues of the Drosophila embryo respond to homeotic gene expression in an immediate and lasting way, much like a "switch," so that further presence of the protein is unnecessary for continued differentiation (Castelli-Gair et al., 1994).

O40 Cytochrome P450

The second gene we identified as being expressed during early ovule development is a member of the cytochrome P450 monooxygenase superfamily. Interestingly, in situ hybridization has shown that O40 transcripts are not specific to ovules but rather are found exclusively in the pollen tubes intertwined with the ovules at these stages of development (Figure 7). This observation underscores the importance and necessity of examining the tissue localization of gene expression before the development of hypotheses concerning the role of the gene product in the plant.

The cytochrome P450 monooxygenases are known to catalyze a wide variety of oxidative reactions in animals, including the metabolism of steroids, biogenic amines, fatty acids, prostaglandins, and leukotrienes, as well as the detoxification of xenobiotic substances (Nebert and Gonzalez, 1987; Nelson et al., 1993). In plants, cytochrome P450 monooxygenases are known to play a role in the biosynthesis of terpenoids, phenylpropanoids, gibberellins, fatty acids, and sterols, as well as in the detoxification of herbicides (Benveniste et al., 1982; O'Keefe et al., 1987; Donaldson and Luster, 1991). Because of the immense variety of possible substrates acted on by cytochrome P450 monooxygenases, it is difficult to predict what the function of O40 might be in the pollen tube. Unfortunately, sequence analysis provides little information about the possible activity of O40 because the most closely related gene, MTC1, also has no known function (Larkin, 1994).

A provocative possibility is that O40 plays a role in the biosynthesis of a hormone involved in intercellular communication, an idea that is certainly not without precedent in animal systems. The most thoroughly studied cytochrome P450 monooxygenases are known to catalyze multiple steps in the metabolism of such steroid hormones as testosterone and estrogen (Nebert and Gonzalez, 1987). Related substances such as androgen and estrogen have been identified tentatively in several plant species (Simons and Grinwich, 1989) and have been suggested to play a role in aspects of reproduction such as sex expression and floral induction, although the evidence

is inconclusive (Kopcewicz, 1970, 1972; Jones and Roddick, 1988; Zhang et al., 1991). However, functions of this class of enzymes in plants may be considerably different from those in animal systems, because this complex gene family is ancient and probably has undergone major functional diversification since the divergence of the plant and animal kingdoms (Nelson et al., 1993).

An exciting possibility is that O40 might play a role in the biosynthesis of nonpolar plant growth substances, as does the recently cloned *Dwarf3* locus (Winkler and Helentjaris, 1995). This gene encodes a cytochrome P450 monooxygenase belonging to a new family (CYP88) thought to catalyze one of the early steps in the biosynthesis of gibberellin (*ent*-kaurene to *ent*-7α-hydroxykaurenoic acid). Alternatively, O40 may play a role in the biosynthesis of plant hormones such as abscisic acid or brassinosteroids. Pollen has long been known to be a rich source of brassinosteroid compounds, but little is known about the biological role of such compounds in pollen (Mandava, 1988). It is clear that brassinosteroids can induce elongation or swelling of tissues as well as cell division when applied to various plant tissues (Mandava, 1988). Recent study of the gibberellin mutant *gib-1* in tomato has shown that gibberellin plays a role in pollen development, because deficiency causes gibberellin-reversible arrest of the pollen mother cells in the G1 phase of the premeiotic interphase (Jacobsen and Olszewski, 1991). It is interesting to speculate that synthesis or modification of a plant hormone by the pollen tube might be important for some aspect of pollen tube elongation or for the continued growth of the ovary and ovules in response to pollination.

Finally, it is possible that the O40 gene product is involved in the biosynthesis of a secondary metabolite found in the pollen tube. Work with chalcone synthase–deficient plants has shown that pollen germination requires the presence of specific flavonols and that male fertility of chalcone synthase–deficient plants can be restored by applying these flavonols to the stigma (Mo et al., 1992). This work showed that secondary metabolites can play a crucial role in developmental events, in this case, pollen hydration and growth.

Late Development

O108

RNA blot hybridization analysis showed that O108 gene expression is limited to 11 WAP, when ovule development is nearly complete. This pattern is substantiated by results from in situ hybridization to immature and mature ovules. Moreover, the pattern of O108 expression is regulated in a cell-specific manner within the ovule itself, so only the outermost layer of the outer integument and the female gametophyte express the gene at detectable levels (Figure 8). This unique spatial pattern of expression suggests that the gene product plays a specific role in processes within the ovule, but the function of the O108 product is not known. It can be concluded logically that nucleotide binding may play a role in the function of the protein, because both O108 and an Arabidopsis EST with which it shares sequence similarity contain a consensus ATP/GTP binding domain.

An interesting observation derived from analysis of this gene is that the domain of O108 expression is not delineated by structurally defined tissues of the ovule. Despite the fact that both layers of the outer integument in the Phalaenopsis ovule are morphologically similar and appear to play the same role in seed ontogeny (Wirth and Withner, 1959), O108 transcripts are found only in the outermost layer of the outer integument. In addition, O108 is expressed in the gametophyte, a tissue that does not, at least at the superficial level, appear to share any obvious morphological or biochemical function with the outer integument. The biochemical "compartments" within the organs of the flower do not necessarily intersect exactly with anatomically recognizable tissues; this information can provide insight into the function of the gene itself as well as point to previously unrecognized biochemical differentiation of subsets of cells (Gasser, 1991).

In this case, the expression domain of O108 led us to speculate that the outermost or epidermal layer of the ovule has a specific role in successful seed production, perhaps by echoing a signal produced by a mature or receptive female gametophyte to attract a pollen tube. It is obvious that signaling between the ovules and the pollen tube must occur, because previous observations have shown that Phalaenopsis pollen tubes, which have been present in the ovary for ~10 weeks, resume elongation and reorient the direction of growth when ovules begin to mature (Zhang and O'Neill, 1993). Additional evidence for the active participation of the ovule in pollen tube attraction is provided by mutants in ovule development in Arabidopsis. Mutants that fail to develop a mature ovule also fail to attract pollen tubes (Hülskamp et al., 1995).

O108 is expressed in tissues during both the diploid sporophytic and the haploid gametophytic phases of the plant life cycle. Common use of the same gene indicates that genes and regulatory mechanisms may be shared between haploid and diploid tissues, rather than being unique to these very different stages of the plant life cycle.

O126 Glycine-Rich Protein

Like O108, O126 (PGRP-1) is expressed exclusively in ovule tissue at 11 WAP, as determined by RNA blot hybridization (Figure 3). This gene encodes a glycine-rich protein distinct from previously reported sequences. Glycine-rich proteins isolated to date fall into three known classes: (1) structural proteins in the cell wall (Keller et al., 1989; Condit et al., 1990; de Oliveira et al., 1990); (2) cytokeratin-like proteins (Rohde et al., 1990); and (3) RNA binding proteins (Crétin and Puigdomènech, 1990; Ludevid et al., 1992; Sturm, 1992). O126 represents a putative cell wall structural protein because it contains a signal peptide that most likely targets it to the extracellular matrix, and it

contains loosely defined sequence repeats common to glycine-rich cell wall proteins (Figure 14). O126 does not contain an RNA binding consensus domain, so it is unlikely to be a member of this class of proteins. On the other hand, the large proportion of acidic residues in the glycine-rich domain of the protein seems to be a unique characteristic of O126 not shared by other basic or highly hydrophobic cell wall structural proteins.

Many characterized glycine-rich proteins are regulated developmentally within the plant (Condit and Meagher, 1987; Condit et al., 1990; de Oliveira et al., 1990, 1993; Ryser and Keller, 1992; Showalter et al., 1992) and may respond to external signals, such as virus infection (de Oliveira et al., 1990; Linthorst et al., 1990; Fang et al., 1991) and light (Sheng et al., 1993) or wounding, drought stress, and abscisic acid treatment (Showalter et al., 1992). In two cases, glycine-rich proteins that have been shown definitively to be present in the cell wall are tissue specific: petunia GRP1 has been localized to the vascular tissue in cells and is most likely present in the cell walls of the phloem or cambium (Condit et al., 1990); *Phaseolus* GRP1.8 has also been localized to the vascular tissue, primarily in the protoxylem cell walls, but immunogold labeling of the Golgi apparatus suggests that the protein is secreted by xylem parenchyma (Ryser and Keller, 1992). In both cases, it is proposed that the protein plays a role in cell wall formation, but in the case of *P. vulgaris*, the protein has recently been shown to be not associated strictly with wall lignification, as hypothesized previously (Ryser and Keller, 1992). Because there is no vascularization in the Phalaenopsis ovule and no expression of O126 in other vascularized tissues of the plant, it is unlikely that O126 has a similar tissue specificity. Instead, it is possible that O126 is a component of a specialized cell wall in the ovule.

O141 Cysteine Proteinase

RNA gel blot hybridization demonstrated that O141 transcripts were expressed in ovule tissue only at 11 WAP, when ovule development is complete (Figure 3). This pattern of expression is defined further by in situ hybridization, which shows that transcripts are present only in mature ovules (Figure 10). Moreover, expression was limited to the outer integument of the ovule after the outer integument had elongated to its full length. We suggest that O141 may be involved in the late stages of biochemical differentiation of the outer integument. The similarity between the putative O141 product and cysteine proteinases (Cysps) provides some insight into the function of this gene.

The O141 polypeptide is most similar to the papain family of Cysps found in seed or fruit of several species. O141 has the most similarity with a subgroup of papain-like cysteine proteinases, including the *V. mungo* protein that is induced during seed germination and is thought to be involved in seed storage protein degradation (Akasofu et al., 1989; Mitsuhashi and Minamikawa, 1989). Similarly, O141 bears significant similarity with EP-C1 from *P. vulgaris* pods (Tanaka et al., 1991), which has been hypothesized to play a role in the mobilization of amino acids from proteins in the maturing pod to the developing seed. O141 bears significant but considerably less similarity with monocot seed storage mobilization proteins such as aleurain and EP-B from barley (Rogers et al., 1985; Koehler and Ho, 1988) and oryzains from rice (Watanabe et al., 1991). O141 is not expressed in maturing or germinating seed or in the orchid fruit wall, however, making it unlikely that it is involved in storage protein mobilization.

O141 is similar to the well-characterized Cysps papain and actinidin, which are found in fruit tissues (Cohen et al., 1986; Praekelt et al., 1988). The function of these proteins is not understood, but they may be involved in defense against herbivores. It seems unlikely that O141 plays a similar role, because it is not expressed in the ovary wall and because the window of expression during development is very limited. It also seems unlikely that O141 is involved in stress responses, as has been observed for several other related Cysps with a somewhat lower degree of similarity. These Cysps are induced after wounding (Linthorst et al., 1993), cold shock (Schaffer and Fischer, 1988), drought, or wilting stress (Guerrero et al., 1990; Koizumi et al., 1993; Williams et al., 1994).

A potential role of O141 in the biochemical specialization of the integument might be the production of a mobile signal that acts to attract chemotropically the growing pollen tube to a receptive ovule. This possibility is intriguing in light of studies demonstrating that several polypeptide hormones and neuropetides in animal systems are cleaved by specific Cysp activities to yield a biologically active peptide. For example, the conversion of proinsulin to insulin is performed by a 31.5-kD Cysp (Docherty et al., 1982). A Cysp also has been implicated in the conversion of β-endorphin precursor by the rat pituitary intermediate lobe (Loh and Gainer, 1982). In these cases, the Cysp activity is regulated developmentally so that the activation of a precursor peptide occurs under the appropriate conditions. These observations led us to speculate that a possible function of O141 might be the specific cleavage of a pro-hormone that is released at ovule maturity and that attracts the growing pollen tube to the ovule.

Alternatively, O141 might act to degrade the set of proteins associated with the young integument to allow the integument to install a new set of proteins associated with the biochemical processes necessary for the conversion of the outer integument to the mature seed coat. A similar role has been proposed for the developmentally regulated cysteine proteinase 1 of Dictyostelium; in this case, the proteinase activity may be associated with bulk protein degradation for nutrition before stalk formation or in targeted degradation of developmentally significant proteins during the shift from slime to stalk development (Williams et al., 1985).

One obvious event in the formation of the seed coat is the degeneration of integument cells. This event occurs relatively early in the formation of the orchid seed because of its reduced nature; the embryo undergoes very little development before seed maturity, and there is little growth and differentiation of other

seed structures after fertilization (Wirth and Withner, 1959). Because the time at which integument cells die corresponds with the window of O141 gene expression, it is conceivable that O141 plays a role in conducting the developmentally programmed cell death. This idea is supported by the developmental pattern of expression of TA56, a Cysp isolated from tobacco (Koltunow et al., 1990). This gene is expressed only in the anther, initially in the circular cluster of cells between the stomium and connective and later in the connective and stomium. In these locations, expression of TA56 immediately precedes degradation of cells that allow the anther to dehisce and release the pollen grains.

Furthermore, this idea is lent credence by the recent realization that cysteine proteinases play a role in regulating programmed cell death in animals. The mammalian interleukin-1β–converting enzyme (ICE) is a Cysp (Vaux et al., 1994) that seems to be both necessary and sufficient to induce apoptosis in rat fibroblasts (Miura et al., 1993). In addition, the gene *Ced-3* that is required for apoptosis in *Caenorhabditis elegans* encodes an ICE homolog (Yuan et al., 1993). When these proteins are active, apoptosis probably results from degradation of a protein(s) necessary for cellular function. Although O141 does not share sequence similarity with the ICE/Ced-3 family of Cysps, the functional similarity is provocative, and thus it is interesting to speculate that the activity of specific Cysps might be tied to programmed cell death in the integument.

Genetic Control of Ovule Development Can Be Generalized from Orchids to Other Plant Species

In conclusion, the unique physiology of orchid flowers has provided the basis for the identification of stage- and tissue-specific molecular events in ovule development, but unfortunately, this system is not suitable for genetic mutant analysis or for the routine production of transgenic plants. Because the primary future goal of our research is to elucidate the function of several ovule stage–specific genes, it is important for information and genes derived from orchids to be transferred to another more tractable genetic system, such as Arabidopsis. Although orchid flowers are unusual in that ovule development is delayed and triggered by pollination, once initiated, the processes of megasporogenesis and megagametogenesis are similar to those in many other flowering plant species, with the development of the mature female gametophyte being of the Polygonum type (Figure 1). Recently, we found that transcripts homologous to orchid ovule stage–specific genes are present in Arabidopsis flower buds (J.A. Nadeau and S.D. O'Neill, unpublished results). Taken together, it appears likely that the molecular tools developed in orchids to study ovule development can be used to isolate homologous genes from Arabidopsis to test their function in a system better suited to genetic analysis. In addition, it is likely that the information derived from both species will be transferable to a wide range of crop species that share similar aspects of ovule and female gametophyte development.

METHODS

Plant Material

Genetically identical orchid plants of the genus *Phalaenopsis* (cv SM9108; Stewart Orchids, Carpinteria, CA) that were generated by mericloning were used for all material in this study. Plants were maintained under optimal growth conditions in the greenhouse at the University of California–Davis. Flowers from these plants were pollinated randomly, and ovaries were harvested at appropriate times after pollination. After each harvest, tissues were frozen immediately in liquid nitrogen. A small sample of tissue from each time point was examined whole by light microscopy to confirm the stage of ovule development.

Tissues harvested at 0, 1, and 4 weeks after pollination (WAP) contained both ovary wall and meristematic ovule and placental tissues, which could not be separated due to the early stage of ovule development. Tissues harvested subsequently were separated into ovules and ovary wall by rapid dissection. The top and bottom of the ovaries were excised and discarded because the ovules at the extreme ends of the ovary were not generally at the same developmental stage; the remaining ~70% of the ovary was opened longitudinally with a sterile razor blade, effectively splitting it into sections representing the three locules. The thin layer of ovules along the placental region of each slice was dissected with a razor blade, taking care to avoid adjacent areas containing numerous hair cells (Zhang and O'Neill, 1993). Most pollen tubes were pulled out of the wall and ovule tissue before freezing, but by 5.5 WAP, many pollen tubes were well intertwined with the ovules and could not be separated without damaging the tissue. The ovary wall tissue, on the other hand, contains hair cells. Young leaves, roots, and unpollinated flower parts also were removed with a sterile razor blade and frozen immediately in liquid nitrogen to represent vegetative and other reproductive organs of the plant.

Library Construction

Total RNA was isolated as described previously (O'Neill et al., 1993). Poly(A)$^+$ RNA was isolated using paramagnetic oligo(dT) beads (Dynabeads; Dynal, Lake Success, NY), according to the manufacturer's suggestions. LiCl was removed from the poly(A)$^+$ RNA by two ethanol precipitations before first-strand cDNA synthesis. Libraries were constructed from 5 μg of poly(A)$^+$ RNA isolated from 5.5-, 6.5-, 7-, and 11-WAP ovule tissue as well as from pollen tube tissue. RNA from 5.5-WAP ovule tissue was used for the archesporial cell–stage library, 11 WAP ovule tissue was used for the mature ovule library, and RNA from 6.5- and 7-WAP ovules was pooled for the construction of the megasporocyte-stage library. cDNA was constructed and cloned into the λZAPII phage vector (Stratagene), according to the manufacturer's protocol. The three ovule cDNA libraries each contained ~3 × 10^6 clones, and the pollen tube cDNA library contained ~1.8 × 10^6 clones, of which ≥95% contained inserts.

Library Screening

Three-way differential screening was conducted with the 6.5-, 7-, and 11-WAP libraries. Approximately 2.0 × 10^5 clones from each library were plated out, and three replica filters (BA85 nitrocellulose; Schleicher & Schuell, Keene, NH) were made from each plate. Each filter set was hybridized with first-strand cDNA probes synthesized from either 6.5-

or 11-WAP ovule poly(A)$^+$ RNA as the experimental probes, or 6.5-WAP combined with 11-WAP ovary wall poly(A)$^+$ RNA as the control probe. cDNAs were labeled with ^{32}P-dATP in 50-μL reverse transcription reactions containing 5 μg of poly(A)$^+$ RNA, 1.5 μg of oligo(dT)$_{12-18}$ (Pharmacia), 40 units of RNasin (Promega), 50 μM dATP, 500 μM dCTP, dGTP, and dTTP, 1 × reverse transcriptase buffer (Gibco BRL), 10 mM DTT, 12.5 μL of α-^{32}P-dATP (6000 Ci/mmol), and 600 units of SuperscriptII reverse transcriptase (Gibco BRL) at 37°C for 1 hr.

DNA and RNA Gel Blot Analyses

The methods used for RNA extraction as well as RNA gel blot hybridization have been described previously (O'Neill et al., 1993), except that 20 μg of total RNA was used in each lane of the RNA gels. DNA was extracted from young leaves, as described by Jofuku and Goldberg (1988). Fifteen micrograms of genomic DNA was digested with EcoRI, BamHI, or HindIII (Promega), according to standard procedures, reprecipitated by the addition of 0.3 M NaCl and 2.5 volumes of 95% ethanol, resuspended in Tris-EDTA, and electrophoresed on a 0.8% agarose gel for 12 hr at 4°C. The DNA was transferred to Nytran membranes (Schleicher & Schuell) by overnight capillary transfer, according to standard procedures (Sambrook et al., 1989).

Both RNA and DNA blots were hybridized with probes labeled to high specific activity by random priming (Prime-a-Gene kit; Promega) with ^{32}P-dCTP, as described previously (O'Neill et al., 1993). RNA gel blots were hybridized at 42°C for 48 hr in 50% formamide, 5 × SSC (1 × SSC is 0.15 M NaCl, 0.015 M sodium citrate), 0.05 M phosphate buffer, pH 6.5, 1 × Denhardt's solution (1 × Denhardt's solution is 0.02% Ficoll, 0.02% PVP, 0.02% BSA), 0.2 mg/mL sheared denatured salmon testes DNA (Type III; Sigma), and 0.2% SDS (Gibco BRL), to which denatured labeled probe was added to a final concentration of 1.5 × 10^6 cpm/mL of hybridization solution. RNA blots were washed once at room temperature for 20 min, twice at 55°C, and once at 63°C for 20 min. Each wash was in 0.2 × SSC, 0.1% SDS, 0.05 M phosphate buffer, pH 6.5. After being stripped, all RNA blots were hybridized with a Phalaenopsis actin clone (GenBank accession number U18102) to confirm the presence of undegraded RNA in each lane.

DNA gel blots were hybridized at 42°C for 48 hr in 50% formamide, 5 × SSC, 0.05 M phosphate buffer, pH 7.0, 5 × Denhardt's solution, 0.2 mg/mL of sheared denatured salmon testes DNA (Type III; Sigma), 0.2% SDS (Gibco BRL), to which denatured labeled probe was added to a final concentration of 5 × 10^6 cpm/mL of hybridization solution. DNA blots were washed once at room temperature for 20 min and twice at 55°C for 20 min; each wash was in 0.2 × SSC, 0.1% SDS, 0.01% sodium pyrophosphate. Autoradiography was performed at −80°C, using Kodak XAR-5 film and one intensifying screen (Cronex Lightning Plus; Du Pont). DNA gel blots were exposed for 2 to 5 days, whereas each RNA gel blot hybridization experiment was exposed to film at least twice. The first exposure, which varied from 12 hr to 4 days, was calculated to be appropriate for photographic reproduction, whereas the final exposure was for 7 to 10 days to detect faint bands not apparent in shorter exposures.

Sequence Analysis

Clones were reconstituted as pBluescript SK− plasmids from the λZAPII library by in vivo excision, as described by the manufacturer's protocol (Stratagene). Sequencing was performed by the dideoxynucleotide chain termination method (Sanger et al., 1977), using Sequenase version 2 as suggested by the manufacturer (U.S. Biochemical/Amersham). Nested deletions were constructed by exodeletion, using the Erase-a-Base system (Promega), and by restriction digestion of the plasmids. In the case of some clones, sequence-specific primers were synthesized and used to generate overlapping sequence information. Sequence analysis and multiple sequence alignment (PILEUP) were accomplished by using Genetics Computer Group (Madison, WI) and BLAST (Altschul et al., 1990) computer programs.

In Situ Hybridization

The fixation and embedding of tissues for in situ hybridization to mRNA in tissue sections was performed as described initially for immunolocalization by Baskin et al. (1992) and described subsequently for detection of mRNA by Kronenberger et al. (1993), with a few modifications. Essentially, 1.0- to 1.5-mm slices of tissue were fixed in 4% paraformaldehyde (Sigma), 0.3% glutaraldehyde (Polysciences, Warrington, PA), and 0.1% Triton X-100 (Sigma) in 0.05 M phosphate buffer, pH 7.0, for 1 to 4 hr at 4°C. Tissue was transferred to fresh fixative overnight and then rinsed three times with buffer alone to remove fixative. Tissue was dehydrated by passage through a graded ethanol series (10 to 100%) containing 1 mM DTT. The tissue was infiltrated with 4:1 (v/v) *N*-butyl-methacrylate:methyl-methacrylate (Ted Pella, Inc., Redding, CA) embedding material without DTT, which proved to be unnecessary and tended to make the resin brittle. The tissue was placed sequentially into 2:1, 1:1, then a 1:2 ethanol–methacrylate mixture (v/v) for at least 12 hr at each step. Finally, tissue was placed into three changes of pure methacrylate solution for 24 hr each, which contained 0.5% benzoin ethyl ether and through which nitrogen gas had been bubbled to displace dissolved oxygen. Tissue was placed in plastic molds (model no. 16643A; Polysciences) with fresh embedding media, covered with parafilm, and exposed to UV light supplied from 20 cm below the mold by a small hand-held long-wave UV source for 12 to 18 hr. All steps were performed at 4°C, and all solutions and materials were made RNase free, according to standard procedures (Sambrook et al., 1989). Tissue was sectioned dry on glass knives with a Reichert-Jung ultramicrotome to 2.5 or 5 μm and placed on drops of distilled water on Superfrost Plus microscope slides (Fisher). Sections were spread with chloroform and allowed to dry onto the slides overnight at 42°C.

Hybridization, washing, and autoradiography were performed as described previously (Nadeau et al., 1993) and as modified from the procedure described originally by Cox and Goldberg (1988), with a few exceptions. Initially, the methacrylate embedding media was removed thoroughly by two washes in 100% acetone for 20 min each, with gentle stirring. Slides were then rinsed three times in water before BSA treatment. Proteinase K digestion was performed essentially as described, except proteinase K (Boehringer Mannheim) was used at 10 μg/mL rather than 1 μg/mL. ^{35}S-UTP–labeled RNA probes were synthesized by in vitro transcription from pBluescript SK− plasmids (Stratagene) by using T7 and T3 RNA polymerases (Promega), as described previously. Probes were purified using diethyl pyrocarbonate–treated Chromaspin-100 columns (Clontech, Palo Alto, CA) and then sheared as described previously (Nadeau et al., 1993). Hybridizations were conducted at 44°C as described previously, except for O39, in which case the hybridization was performed at both 44 and 50°C. Slides were air dried after the hybridization wash steps, and autoradiography was performed as described previously. Slides were exposed for 7 to 21 days, as necessary. Slides were stained subsequently with 0.005% toluidine blue (w/v) in water, passed through an ethanol dehydration

series to xylene, and mounted in Permount (Fisher). An Olympus BX60 microscope was used for bright-field, dark-field, and epifluorescence photography with Kodak color Gold or Ektar film (Kodak).

Microscopy

To visualize intact ovule structure, tissue was harvested directly into clearing solution composed of 1:1:1 chloroform–methyl salicylate–DMSO (v/v). After several hours at 4°C, tissue was mounted in the same media and photographed with differential interference contrast (Nomarski) microscopy, using an Olympus BX50 microscope. Photographs were made with Kodak Gold 400 film.

ACKNOWLEDGMENTS

We thank Elena Lee for technical assistance and Karen English-Loeb for constructing Figure 1. We thank Dr. David Nelson and the P450 Gene Nomenclature Committee for naming CYP78A2. J.A.N. was supported by an American Orchid Society Vaughn-Jordan Fellowship. This research was supported by Grant Nos. 91-37304-6464 and 95-37304-2322 from the U.S. Department of Agriculture National Research Initiative Competitive Grants Program to S.D.O. Facility support was provided by the National Science Foundation Plant Cell Biology Training Grant No. DIR-9014274. We acknowledge the Arabidopsis Biological Resource Center at Ohio State University for the Arabidopsis EST clone.

Received September 20, 1995; accepted December 11, 1995.

REFERENCES

Akasofu, H., Yamauchi, D., Mitsuhashi, W., and Minamikawa, T. (1989). Nucleotide sequence of cDNA for sulfhydryl-endopeptidase (SH-EP) from cotyledons of germinating *Vigna mungo* seedlings. Nucleic Acids Res. **17,** 6733.

Altschul, S.F., Gish, W., Miller, W., Myers, E.W., and Lipman, D.J. (1990). Basic local alignment search tool. J. Mol. Biol. **215,** 403–410.

Baskin, T.I., Busby, C.H., Fowke, L.C., Sammut, M., and Gubler, F. (1992). Improvements in immunostaining samples embedded in methacrylate: Localization of microtubules and other antigens throughout developing organs in plants of diverse taxa. Planta **187,** 405–413.

Bellmann, R., and Werr, W. (1992). Zmhox1a, the product of a novel maize homeobox gene, interacts with the *Shrunken* 26 bp *feedback* control element. EMBO J. **11,** 3367–3374.

Benveniste, I., Gabriac, B., Fonne, R., Reichhart, D., Salaün, J.-P., Simon, A., and Durst, F. (1982). Higher plant cytochrome P-450: Microsomal electron transport and xenobiotic oxidation. In Cytochrome P-450, Biochemistry, Biophysics and Environmental Implications, E. Hietanen, M. Laitinen, and O. Hänninen, eds (Amsterdam, The Netherlands: Elsevier Biomedical Press), pp. 201–208.

Bouman, F. (1984). The ovule. In Embryology of Angiosperms, B.M. Johri, ed (Berlin: Springer-Verlag), pp. 123–157.

Bozak, K.R., Yu, H., Sirevag, R., and Christoffersen, R.E. (1990). Sequence analysis of ripening-related cytochrome P-450 cDNAs from avocado fruit. Proc. Natl. Acad. Sci. USA **87,** 3904–3908.

Castelli-Gair, J., Greig, S., Micklem, G., and Akam, M. (1994). Dissecting the temporal requirements for homeotic gene function. Development **120,** 1983–1995.

Cohen, L.W., Coughlan, V.M., and Dihel, L.C. (1986). Cloning and sequencing of papain-encoding cDNA. Gene **48,** 219–227.

Condit, C.M., and Meagher, R.B. (1986). A gene encoding a novel glycine-rich structural protein of petunia. Nature **323,** 178–181.

Condit, C.M., and Meagher, R.B. (1987). Expression of a gene encoding a glycine-rich protein in petunia. Mol. Cell. Biol. **7,** 4273–4279.

Condit, C.M., McLean, B.G., and Meagher, R.B. (1990). Characterization of the expression of the petunia glycine-rich protein-1 gene product. Plant Physiol. **93,** 596–602.

Cox, K.H., and Goldberg, R.B. (1988). Analysis of plant gene expression. In Plant Molecular Biology: A Practical Approach, C.H. Shaw, ed (Oxford, UK: IRL Press Ltd.), pp. 1–34.

Crétin, C., and Puigdomènech, P. (1990). Glycine-rich RNA-binding proteins from *Sorghum vulgare*. Plant Mol. Biol. **15,** 783–785.

Denecke, J., De Rycke, R., and Botterman, J. (1992). Plant and mammalian sorting signals for protein retention in the endoplasmic reticulum contain a conserved epitope. EMBO J. **11,** 2345–2355.

de Oliveira, D.E., Seurinck, J., Inzé, D., Van Montagu, M., and Botterman, J. (1990). Differential expression of five Arabidopsis genes encoding glycine-rich proteins. Plant Cell **2,** 427–436.

de Oliveira, D.E., Franco, L.O., Simoens, C., Seurinck, J., Coppieters, J., Botterman, J., and Van Montagu, M. (1993). Inflorescence-specific genes from *Arabidopsis thaliana* encoding glycine-rich proteins. Plant J. **3,** 495–507.

Docherty, K., Carroll, R.J., and Steiner, D.F. (1982). Conversion of proinsulin to insulin: Involvement of a 31,500 molecular weight thiol protease. Proc. Natl. Acad. Sci. USA **79,** 4613–4617.

Donaldson, R.P., and Luster, D.G. (1991). Multiple forms of plant cytochrome P-450. Plant Physiol. **96,** 669–674.

Drubin, D.G. (1991). Development of cell polarity in budding yeast. Cell **65,** 1093–1096.

Duboule, D. (1994). Guidebook to the Homeobox Genes. (Oxford: Oxford University Press).

Evans, P.T., and Malmberg, R.L. (1989). Alternative pathways of tobacco placental development: Time of commitment and analysis of a mutant. Dev. Biol. **136,** 273–283.

Fang, R.-X., Pang, Z., Gao, D.-M., Mang, K.-Q., and Chua, N.-H. (1991). cDNA sequence of a virus-inducible, glycine-rich protein gene from rice. Plant Mol. Biol. **17,** 1255–1257.

Gaiser, J.C., Robinson-Beers, K., and Gasser, C.S. (1995). The Arabidopsis *SUPERMAN* gene mediates asymmetric growth of the outer integument of ovules. Plant Cell **7,** 333–345.

Gasser, C.S. (1991). Molecular studies on the differentiation of floral organs. Annu. Rev. Plant Physiol. **42,** 621–649.

Gehring, W.J. (1993). Exploring the homeobox. Gene **135,** 215–221.

Goodwin, T.W., and Mercer, E.I. (1988). Introduction to Plant Biochemistry. (Oxford, UK: Pergamon Press).

Guerrero, F.D., Jones, J.T., and Mullet, J.E. (1990). Turgor-responsive gene transcription and RNA levels increase rapidly when pea shoots are wilted. Sequence and expression of three inducible genes. Plant Mol. Biol. **15,** 11–26.

Hartings, H., Maddaloni, M., Lazzaroni, N., Di Fonzo, N., Motto, M., Salamini, F., and Thompson, R. (1989). The *O2* gene which regulates zein deposition in maize endosperm encodes a protein with structural homologies to transcriptional activators. EMBO J. **8,** 2795–2801.

Hinnebusch, A.G. (1990). Involvement of an initiation factor and protein phosphorylation in translational control of *GCN4* mRNA. Trends Biochem. Sci. **15,** 148–152.

Holton, T.A., Brugliera, F., Lester, D.R., Tanaka, Y., Hyland, C.D., Menting, J.G.T., Lu, C.-Y., Farcy, E., Stevenson, T.W., and Cornish, E.C. (1993). Cloning and expression of cytochrome P450 genes controlling flower colour. Nature **366,** 276–279.

Huang, B.-Q., and Russell, S.D. (1992). Female germ unit: Organization, isolation, and function. Int. Rev. Cytol. **140,** 233–293.

Hülskamp, M., Schneitz, K., and Pruitt, R.E. (1995). Genetic evidence for a long-range activity that directs pollen tube guidance in Arabidopsis. Plant Cell **7,** 57–64.

Jackson, D., Veit, B., and Hake, S. (1994). Expression of maize *KNOTTED1* related homeobox genes in the shoot apical meristem predicts patterns of morphogenesis in the vegetative shoot. Development **120,** 405–413.

Jacobsen, S.E., and Olszewsi, N.E. (1991). Characterization of the arrest in anther development associated with gibberellin deficiency of the *gib*-1 mutant of tomato. Plant Physiol. **97,** 409–414.

Jofuku, K.D., and Goldberg, R.B. (1988). Analysis of plant gene structure. In Plant Molecular Biology: A Practical Approach, C.H. Shaw, ed (Oxford, UK: IRL Press Limited), pp. 37–66.

Jones, J.L., and Roddick, J.G. (1988). Steroidal estrogens and androgens in relation to reproductive development in higher plants. J. Plant Physiol. **133,** 510–518.

Joppa, L.R., Williams, N.D., and Maan, S.S. (1987). The chromosomal location of a gene (*msg*) affecting megasporogenesis in durum wheat. Genome **29,** 578–581.

Kalinski, A., Weisemann, J.M., Matthews, B.F., and Herman, E.M. (1990). Molecular cloning of a protein associated with soybean seed oil bodies that is similar to thiol proteases of the papain family. J. Biol. Chem. **265,** 13843–13848.

Kamalay, J.C., and Goldberg, R.B. (1980). Regulation of structural gene expression in tobacco. Cell **19,** 935–946.

Kamalay, J.C., and Goldberg, R.B. (1984). Organ-specific nuclear RNAs in tobacco. Proc. Natl. Acad. Sci. USA **81,** 2801–2805.

Kamphuis, I.G., Drenth, J., and Baker, E.N. (1985). Thiol proteases. Comparative studies based on the high-resolution structures of papain and actinidin, and on amino acid sequence information for cathepsins B and H, and stem bromelain. J. Mol. Biol. **182,** 317–329.

Keller, B., Sauer, N., and Lamb, C.J. (1988). Glycine-rich cell wall proteins in bean: Gene structure and association of the protein with the vascular system. EMBO J. **7,** 3625–3633.

Keller, B., Templeton, M.D., and Lamb, C.J. (1989). Specific localization of a plant cell wall glycine-rich protein in protoxylem cells of the vascular system. Proc. Natl. Acad. Sci. USA **86,** 1529–1533.

Koehler, S., and Ho, T.-H.D. (1988). Purification and characterization of gibberellic acid-induced cysteine endoproteases in barley aleurone layers. Plant Physiol. **87,** 95–103.

Koizumi, M., Yamaguchi-Shinozaki, K., Tsuji, H., and Shinozaki, K. (1993). Structure and expression of two genes that encode distinct drought-inducible cysteine proteinases in *Arabidopsis thaliana*. Gene **129,** 175–182.

Koltunow, A.M., Truettner, J., Cox, K.H., Wallroth, M., and Goldberg, R.B. (1990). Different temporal and spatial gene expression patterns occur during anther development. Plant Cell **2,** 1201–1224.

Kopcewicz, J. (1970). Influence of estrogens on flower formation in *Cichorium intybus* L. Naturwissenschaften **57,** 136.

Kopcewicz, J. (1972). Estrogens in the short-day plants *Perilla ocimoides* and *Chenopodium rubrum* grown under inductive and non-inductive light conditions. Z. Pflanzenphysiol. **67,** 373–376.

Korfhage, U., Trezzini, G.F., Meier, I., Hahlbrock, K., and Somssich, I.E. (1994). Plant homeodomain protein involved in transcriptional regulation of a pathogen defense-related gene. Plant Cell **6,** 695–708.

Kronenberger, J., Desprez, T., Höfte, H., Caboche, M., and Traas, J. (1993). A methacrylate embedding procedure developed for immunolocalization on plant tissues is also compatible with in situ hybridization. Cell Biol. Int. Rep. **17,** 1013–1021.

Larkin, J. (1994). Isolation of a cytochrome P450 homologue preferentially expressed in developing inflorescences of *Zea mays*. Plant Mol. Biol. **25,** 343–353.

Lawrence, P.A., and Morata, G. (1994). Homeobox genes: Their function in Drosophila segmentation and pattern formation. Cell **78,** 181–189.

Lei, M., and Wu, R. (1991). A novel glycine-rich cell wall protein gene in rice. Plant Mol. Biol. **16,** 187–198.

Léon-Kloosterziel, K.M., Keijzer, C.J., and Koorneef, M. (1994). A seed shape mutant of Arabidopsis that is affected in integument development. Plant Cell **6,** 385–392.

Linthorst, H.J.M., van Loon, L.C., Memelink, J., and Bol, J.F. (1990). Characterization of cDNA clones for a virus inducible, glycine-rich protein from petunia. Plant Mol. Biol. **15,** 521–523.

Linthorst, H.J.M., van der Does, C., Brederode, F.T., and Bol, J.F. (1993). Circadian expression and induction by wounding of tobacco genes for cysteine proteinase. Plant Mol. Biol. **21,** 685–694.

Loh, Y.P., and Gainer, H. (1982). Characterization of pro-opiocortin–converting activity in purified secretory granules from rat pituitary neurointermediate lobe. Proc. Natl. Acad. Sci. USA **79,** 108–112.

Ludevid, M.D., Freire, M.A., Gómez, J., Burd, C.G., Albericio, F., Giralt, E., Dreyfuss, G., and Pagès, M. (1992). RNA binding characteristics of a 16 kDa glycine-rich protein from maize. Plant J. **2,** 999–1003.

Maheshwari, P. (1950). An Introduction to the Embryology of Angiosperms. (New York: McGraw Hill).

Mandava, N.B. (1988). Plant growth–promoting brassinosteroids. Annu. Rev. Plant Physiol. **39,** 23–52.

Martin, S.J., Green, D.R., and Cotter, T.G. (1994). Dicing with death: Dissecting the components of the apoptosis machinery. Trends Biochem. Sci. **19,** 26–30.

Meyerowitz, E.M., and Somerville, C.R. (1994). *Arabidopsis*. Cold Spring Harbor Monograph Series. (Plainview, NY: Cold Spring Harbor Laboratory Press).

Mitsuhashi, W., and Minamikawa, T. (1989). Synthesis and post-translational activation of sulfhydryl-endopeptidase in cotyledons of germinating *Vigna mungo* seeds. Plant Physiol. **89,** 274–279.

Miura, M., Zhu, H., Rotello, R., Hartwieg, E.A., and Yuan, J. (1993). Induction of apoptosis in fibroblasts by IL-1β–converting enzyme, a mammalian homolog of the C. elegans cell death gene *ced-3*. Cell **75,** 653–660.

Mizutani, M., Ward, E., DiMaio, J., Ohta, D., Ryals, J., and Sato, R. (1993). Molecular cloning and sequencing of a cDNA encoding

mung bean cytochrome P450 (P450C4H) possessing cinnamate 4-hydroxylase activity. Biochem. Biophys. Res. Commun. **190,** 875–880.

Mo, Y.Y., Nagel, C., and Taylor, L.P. (1992). Biochemical complementation of chalcone synthase mutants defines a role for flavonols in functional pollen. Proc. Natl. Acad. Sci. USA **89,** 7213–7217.

Modrusan, Z., Reiser, L., Feldmann, K.A., Fischer, R.L., and Haughn, G.W. (1994). Homeotic transformation of ovules into carpel-like structures in Arabidopsis. Plant Cell **6,** 333–349.

Nadeau, J.A., Zhang, X.S., Nair, H., and O'Neill, S.D. (1993). Temporal and spatial regulation of 1-aminocylopropane-1-carboxylate oxidase in the pollination-induced senescence of orchid flowers. Plant Physiol. **103,** 31–39.

Nebert, D.W., and Gonzalez, F.J. (1987). P450 genes: Structure, evolution, and regulation. Annu. Rev. Biochem. **56,** 945–993.

Nelson, D.R., Kamataki, T., Waxman, D.J., Guengerich, F.P., Estabrook, R.W., Feyereisen, R., Gonzalez, F.J., Coon, M.J., Gunsalus, I.C., Gotoh, O., Okuda, K., and Nebert, D.W. (1993). The P450 superfamily: Update on new sequences, gene mapping, accession numbers, early trivial names of enzymes, and nomenclature. DNA Cell Biol. **12,** 1–51.

Noher de Halac, I., and Harte, C. (1985). Cell differentiation during megasporogenesis and megagametogenesis. Phytomorphology **35,** 189–200.

Obokata, J., Ohme, M., and Hayashida, N. (1991). Nucleotide sequence of a cDNA clone encoding a putative glycine-rich protein 19.7 kDa in *Nicotiana sylvestris.* Plant Mol. Biol. **17,** 953–955.

O'Keefe, D.P., Romesser, J.A., and Leto, K.J. (1987). Plant and bacterial cytochromes P450: Involvement in herbicide metabolism. In Phytochemical Effects of Environmental Compounds, J.A. Saunders, L. Kosak-Channing, and E.E. Conn, eds (New York: Plenum Press), pp. 151–173.

O'Neill, S., Nadeau, J.A., Zhang, X.S., Bui, A.Q., and Halevy, A.H. (1993). Interorgan regulation of ethylene biosynthetic genes by pollination. Plant Cell **5,** 419–432.

Parrott, W.A., and Hanneman, R.E., Jr. (1988). Megasporogenesis in normal and synaptic-mutant (*sy-2*) of *Solanum commersonii* Dun. Genome **30,** 536–539.

Praekelt, U.M., McKee, R.A., and Smith, H. (1988). Molecular analysis of actinidin, the cysteine proteinase of *Actinidia chinensis.* Plant Mol. Biol. **10,** 193–202.

Quigley, F., Villiot, M.-L., and Mache, R. (1991). Nucleotide sequence and expression of a novel glycine-rich protein gene from *Arabidopsis thaliana.* Plant Mol. Biol. **17,** 949–952.

Rédei, G. (1965). Non-Mendelian megagametogenesis in *Arabidopsis.* Genetics **51,** 857–872.

Reiser, L., and Fischer, R.L. (1993). The ovule and embryo sac. Plant Cell **5,** 1291–1301.

Rerie, W.G., Feldmann, K.A., and Marks, M.D. (1994). The *GLABRA2* gene encodes a homeodomain protein required for normal trichome development. Genes Dev. **8,** 1388–1399.

Robinson-Beers, K., Pruitt, R.E., and Gasser, C.S. (1992). Ovule development in wild-type Arabidopsis and two female-sterile mutants. Plant Cell **4,** 1237–1249.

Rogers, J.C., Dean, D., and Heck, G.R. (1985). Aleurain: A barley thiol protease closely related to mammalian cathepsin H. Proc. Natl. Acad. Sci. USA **82,** 6512–6516.

Rohde, W., Rosch, K., Kröger, K., and Salamini, F. (1990). Nucleotide sequence of a *Hordeum vulgare* gene encoding a glycine-rich protein with homology to vertebrate cytokeratins. Plant Mol. Biol. **14,** 1057–1059.

Ruberti, I., Sessa, G., Lucchetti, S., and Morelli, G. (1991). A novel class of plant proteins containing a homeodomain with a closely linked leucine zipper motif. EMBO J. **10,** 1787–1791.

Ryser, U., and Keller, B. (1992). Ultrastructural localization of a bean glycine-rich protein in unlignified primary walls of protoxylem cells. Plant Cell **4,** 773–783.

Sambrook, J., Fritsch, E.F., and Maniatis, T. (1989). Molecular Cloning: A Laboratory Manual, 2nd ed. (Cold Spring Harbor, NY: Cold Spring Harbor Laboratory Press).

Sandal, N.N., Bojsen, K., Richter, H., Sengupta-Gopalan, C., and Marcker, K.A. (1992). The nodulin 24 protein family shows similarity to a family of glycine-rich plant proteins. Plant Mol. Biol. **18,** 607–610.

Sanger, F., Nickleu, S., and Coulson, A.R. (1977). DNA sequencing with chain terminating inhibitors. Proc. Natl. Acad. Sci. USA **74,** 5463–5467.

Schaffer, M.A., and Fischer, R.L. (1988). Analysis of mRNAs that accumulate in response to low temperature identifies a thiol protease gene in tomato. Plant Physiol. **87,** 431–436.

Schena, M., and Davis, R.W. (1992). HD-Zip proteins: Members of an *Arabidopsis* homeodomain protein superfamily. Proc. Natl. Acad. Sci. USA **89,** 3894–3898.

Schindler, U., Beckmann, H., and Cashmore, A.R. (1993). HAT3.1, a novel *Arabidopsis* homeodomain protein containing a conserved cysteine-rich region. Plant J. **4,** 137–150.

Scott, M.P., Tamkun, J.W., and Hartzell, G.W., III (1989). The structure and function of the homeodomain. Biochim. Biophys. Acta **989,** 25–48.

Sheng, J., Jeong, J., and Mehdy, M.C. (1993). Developmental regulation and phytochrome-mediated induction of mRNAs encoding a proline-rich protein, glycine-rich proteins, and hydroxyproline-rich glycoproteins in *Phaseolus vulgaris* L. Proc. Natl. Acad. Sci. USA **90,** 828–832.

Showalter, A.M., Butt, A.D., and Kim, S. (1992). Molecular details of tomato extensin and glycine-rich protein gene expression. Plant Mol. Biol. **19,** 205–215.

Simons, R.G., and Grinwich, D.L. (1989). Immunoreactive detection of four mammalian steroids in plants. Can. J. Bot. **67,** 288–296.

Singh, K., Dennis, E.S., Ellis, J.G., Llewellyn, D.J., Tokuhisa, J.G., Wahleithner, J.A., and Peacock, W.J. (1990). OCSBF1, a maize Ocs enhancer binding factor: Isolation and expression during development. Plant Cell **2,** 891–903.

Stinson, J.R., Eisenberg, A.J., Willing, R.P., Pe, M.E., Hanson, D.D., and Mascarehas, J.P. (1987). Genes expressed in the male gametophyte of flowering plants and their isolation. Plant Physiol. **83,** 442–447.

St. Johnson, D., and Nüsslein-Volhard, C. (1992). The origin of pattern and polarity in the *Drosophila* embryo. Cell **68,** 210–219.

Sturm, A. (1992). A wound-inducible glycine-rich protein from *Daucus carota* with homology to single-stranded nucleic acid-binding proteins. Plant Physiol. **99,** 1689–1692.

Tanaka, T., Yamauchi, D., and Minamikawa, T. (1991). Nucleotide sequence of cDNA for an endopeptidase (EP-C1) from pods of maturing *Phaseolus vulgaris* fruits. Plant Mol. Biol. **16,** 1083–1084.

Teutsch, H.G., Hasenfratz, M.P., Lesot, A., Stoltz, C., Garnier, J.-M., Jeltsch, J.-M., Durst, F., and Werk-Reichhart, D. (1993). Isolation and sequence of a cDNA encoding the Jerusalem artichoke cinnamate 4-hydroxylase, a major plant cytochrome P450 involved in the general phenylpropanoid pathway. Proc. Natl. Acad. Sci. USA **90,** 4102–4106.

Ursin, V.M., Yamaguchi, J., and McCormick, S. (1989). Gametophytic and sporophytic expression of anther-specific genes in developing tomato anthers. Plant Cell **1,** 727–736.

Vaux, D.L., Haecker, G., and Strasser, A. (1994). An evolutionary perspective of apoptosis. Cell **76,** 777–779.

Vollbrecht, E., Veit, B., Sinha, N., and Hake, S. (1991). The developmental gene *Knotted-1* is a member of a maize homeobox gene family. Nature **350,** 241–243.

von Heijne, G. (1986). A new method for predicting signal sequence cleavage sites. Nucleic Acids Res. **14,** 4683–4690.

Watanabe, H., Abe, K., Emori, Y., Hosoyama, H., and Arai, S. (1991). Molecular cloning and gibberellin-induced expression of multiple cysteine proteinases of rice seeds (Oryzains). J. Biol. Chem. **266,** 16897–16902.

Willemse, M.T.M., and van Went, J.L. (1984). The female gametophyte. In Embryology of Angiosperms, B.M. Johri, ed (Berlin: Springer-Verlag), pp. 159–196.

Williams, J., Bulman, M., Huttly, A., Phillips, A., and Neill, S. (1994). Characterization of a cDNA from *Arabidopsis thaliana* encoding a potential thiol protease whose expression is induced independently by wilting and abscisic acid. Plant Mol. Biol. **25,** 259–270.

Williams, J.G., North, M.J., and Mahbubani, H. (1985). A developmentally regulated cysteine proteinase in *Dictyostelium discoideum*. EMBO J. **4,** 999–1006.

Winkler, R.G., and Helentjaris, T. (1995). The maize *Dwarf3* gene encodes a cytochrome P450-mediated early step in gibberellin biosynthesis. Plant Cell **7,** 1307–1317.

Wirth, M., and Withner, C.L. (1959). Embryology and development in the Orchidaceae. In The Orchids: A Scientific Survey, C.L. Withner, ed (New York: Ronald Press Co.), pp. 155–188.

Yuan, J., Shaham, S., Ledoux, S., Ellis, H.M., and Horvitz, H.R. (1993). The C. elegans cell death gene *ced-3* encodes a protein similar to mammalian interleukin-1β-converting enzyme. Cell **75,** 641–652.

Zhang, J.S., Yang, Z.H., and Tsao, T.H. (1991). The occurrence of estrogens in relation to reproductive processes in flowering plants. Sex. Plant Reprod. **4,** 193–196.

Zhang, X.S., and O'Neill, S.D. (1993). Ovary and gametophyte development are coordinately regulated by auxin and ethylene following pollination. Plant Cell **5,** 403–418.